


## RESEARCH ARTICLE

# Transcriptional network analysis in frontal cortex in Lewy body diseases with focus on dementia with Lewy bodies

Gabriel Santpere<sup>1,2\*</sup>, Paula Garcia-Esparcia<sup>3\*</sup>, Pol Andres-Benito<sup>3</sup>, Belen Lorente-Galdos<sup>1,2</sup>, Arcadi Navarro<sup>2,4,5,6</sup>, Isidro Ferrer <sup>3,7,8,9</sup>

<sup>1</sup> Department of Neurobiology, Yale School of Medicine, New Haven, CT.

<sup>2</sup> Department of Experimental and Health Sciences, IBE, Institute of Evolutionary Biology, Universitat Pompeu Fabra-CSIC, Barcelona, Spain.

<sup>3</sup> Department of Pathology and Experimental Therapeutics, University of Barcelona, L'Hospitalet de Llobregat, Spain.

<sup>4</sup> Institute of Science and Technology, Centre for Genomic Regulation (CRG), Barcelona, Spain.

<sup>5</sup> National Institute for Bioinformatics (INB), Barcelona, Spain.

<sup>6</sup> Institució Catalana de Recerca i Estudis Avançats (ICREA), Barcelona, Spain.

<sup>7</sup> Institute of Neuropathology, Service of Pathologic Anatomy, IDIBELL-Hospital Universitari de Bellvitge, Hospitalet de Llobregat, Spain.

<sup>8</sup> Institute of Neurosciences, University of Barcelona, Hospitalet de Llobregat, Spain.

<sup>9</sup> CIBERNED, Network Centre for Biomedical Research of Neurodegenerative Diseases, Institute Carlos III, Spain.

## Keywords

axonema, cerebral cortex, chaperones, dementia with Lewy bodies, dynein, GABA, Lewy body diseases, mitochondria, neurotransmission, purine metabolism, synapses, taste receptors, transcriptome.

## Corresponding author:

Isidro Ferrer, Department of Pathology and Experimental Therapeutics, University of Barcelona, campus Bellvitge, c Feixa LLarga sn, 08097 Hospitalet de Llobregat, Spain (E-mail: 8082ifa@gmail.com)

Received 25 January 2017

Accepted 15 March 2017

Published Online Article Accepted

21 March 2017

\*Authors contributed equally to this work.

Compliance with ethical standards No relevant data; no conflicts of interest.

doi:10.1111/bpa.12511

## Abstract

The present study investigates global transcriptional changes in frontal cortex area 8 in incidental Lewy Body disease (iLBD), Parkinson disease (PD) and Dementia with Lewy bodies (DLB). We identified different coexpressed gene sets associated with disease stages, and gene ontology categories enriched in gene modules and differentially expressed genes including modules or gene clusters correlated to iLBD comprising upregulated dynein genes and taste receptors, and downregulated innate inflammation. Focusing on DLB, we found modules with genes significantly enriched in functions related to RNA and DNA production, mitochondria and energy metabolism, purine metabolism, chaperone and protein folding system and synapses and neurotransmission (particularly the GABAergic system). The expression of more than fifty selected genes was assessed with real time quantitative polymerase chain reaction. Our findings provide, for the first time, evidence of molecular cortical alterations in iLBD and involvement of several key metabolic pathways and gene hubs in DLB which may underlie cognitive impairment and dementia.

## INTRODUCTION

Lewy body diseases (LBDs), which include Parkinson's disease (PD) and dementia with Lewy Bodies (DLB), are neurodegenerative disorders, characterized by the presence of intracytoplasmic neuronal inclusions named Lewy bodies (LB) and abnormal neurites containing  $\alpha$ -synuclein species and aggregates (32, 41, 46, 49, 64). Nonmotor symptoms such as sleep disorders, loss of olfaction and autonomic alterations may precede the appearance of motor symptoms; cognitive impairment and dementia can occur at advanced stages of PD, and dementia is compulsory in DLB. Braak stages of  $\alpha$ -synuclein pathology distribution are useful to delineate a framework to interlink LBDs into a spectrum. Stages 1–3 can be

associated with pre-motor symptoms although in most cases the presence of LBs and neurites in selected regions of the medulla oblongata, pons and midbrain is an incidental finding at autopsy. The term incidental PD or Lewy Body disease (LBD) (iPD or incidental LBD [iLBD]) refers to those early stages of LBD pathology with no apparent clinical symptoms, corresponding to the early stages of LBD spectrum (22). PD is usually manifested at stages 4 and 5 once the involvement of the substantia nigra reaches determine thresholds of neuronal loss and dopaminergic denervation of the striatum is manifested. Cognitive impairment can be detected at stages 5 and 6 in PD, whereas DLB cases are categorized as Braak stages 5 and 6 of LB pathology (11, 84). However, no exact

correlation exists between Braak stages and clinical symptoms linked to cognitive impairment and dementia (14, 23, 28, 47, 48, 65, 77), this fact suggesting that factors other than LBs and neurites play a cardinal role in the pathogenesis of LBDs. Concomitant pathologies, particularly those linked to Alzheimer's disease (AD), have also been suggested to explain variations in the degree of cognitive impairment in DLB (8, 17, 47, 50, 70, 71).

Decreased dopaminergic, noradrenergic serotonergic and cholinergic innervation of the cerebral cortex are contributory factors to the appearance of cognitive impairment and dementia in PD. They are due to the loss of vulnerable neurons in the substantia nigra, locus coeruleus, raphe nuclei and nuclei of the basal forebrain including the basal nucleus of Meynert, respectively (13, 43, 45, 53, 54, 62, 89). However, recent studies demonstrate the primary impairment of several metabolic pathways in the cerebral cortex in PD and other LBDs, such as synaptic transmission, mitochondria and energy metabolism, purine metabolism, protein synthesis, lipid composition of membranes and inflammation, among others (19, 20, 26, 28, 31, 34–36, 61, 63, 68, 74, 79, 94).

Studies of transcriptomic profiling in LBDs have been mainly focused on the typically affected subcortical regions such as substantia nigra, locus coeruleus and striatum in PD (7, 18, 40). Cortical regions have received much less attention with studies limiting their outcome to lists of differentially expressed genes (DEGs) (59). Still, this approach has allowed the discovery of the brain expression of olfactory and taste receptors and their deregulation in the cerebral cortex and substantia nigra in PD (33, 42).

Here, we set out to investigate global transcriptomic changes occurring in the frontal cortex of cases of iLBD, PD and DLB relative to middle-aged individuals with no neurological symptoms and with no alterations at the postmortem examination. We focused particularly on identifying gene coexpression modules showing correlation with the spectrum of LB disorders. By applying weighted gene coexpression network analysis (WGCNA) (57) to microarray data, we determined the transcriptome structure in the frontal cortex and identified coexpression modules correlated to iLBD, PD and DLB. Validation of hubs and selected altered pathways was carried out with real time quantitative polymerase chain reaction (RT-qPCR).

## MATERIAL AND METHODS BRAIN SAMPLES

Brain tissue was obtained from the Institute of Neuropathology Brain Bank (HUB-ICOIDIBELL Biobank) and the Hospital Clinic-IDIBAPS Biobank following the guidelines of Spanish legislation on this matter and of the local ethics committee. Processing of brain tissue has been detailed elsewhere (29, 80). The postmortem interval between death and tissue processing was between 3 h and 15 h. One hemisphere was cut in 1-cm-thick coronal sections, and selected areas of the encephalon were rapidly dissected, frozen on metal plates over dry ice, placed in individual air-tight plastic bags, numbered with water-resistant ink and stored at  $-80^{\circ}\text{C}$  until use for biochemical studies. The other hemisphere was fixed by immersion in 4% buffered formalin for 3 weeks for morphologic studies. Neuropathological diagnosis was categorized following current staging classifications for LBD (1, 10, 78). For AD-related pathology, neurofibrillary tangles (NFTs) (9) and phases of AD-related  $\beta$ -

amyloid plaques (91) were assigned. Only cases with "typical" staging of LBD pathology were selected for study.

Two series of cases were used. The first one served for microarray studies. RNA samples from frontal cortex (area 8) of middle aged (MA) ( $n = 8$ , 4 men, 4 women; age:  $67.5 \pm 12.8$  years), iLBD ( $n = 4$ , 1 men, 3 women; age:  $71.2 \pm 4.5$  years), PD ( $n = 8$ , 4 men, 4 women, age:  $67.8 \pm 8.8$  years) and DLB ( $n = 8$ , 5 men, 3 women; age:  $72.3 \pm 8.6$ ) cases were analyzed using the Affymetrix microarray platform and the Genechip Human Gene 1.1 ST Array (Affymetrix, Santa Clara, CA, USA). The second series of cases was used for RT-qPCR validation of altered expression of selected genes. Cases used for gene validation were iLBD ( $n = 5$ , 4 men, 1 woman; age:  $66.8 \pm 8.9$  years) at stages 3 and 4, and PD cases ( $n = 9$ , 3 men, 6 women; age:  $77.1 \pm 4.7$  years) at stages 5 and 6, DLB cases ( $n = 9$ , 8 men, 1 woman; age:  $76.44 \pm 5.77$  years). PD cases had suffered from parkinsonism and had received treatment during the duration of the disease but did not have dementia. MA cases had not suffered from neurological disease and the neuropathological examination did not reveal abnormalities ( $n = 15$ , 6 men, 9 women, age:  $64.4 \pm 15.5$  years). In addition, four cases with rapid clinical course DLB (rapid course DLB [rpDLB]; two years of less of disease duration) (2 men and 2 women, age:  $73.7 \pm 2.2$  years) were chosen for a few selective studies (37, 38).

Cases with associated pathologies such as vascular diseases (excepting mild atherosclerosis and arteriolosclerosis), TDP-43 proteinopathy, infection of the nervous system, brain neoplasms, systemic and central immune diseases, metabolic syndrome and hypoxia were excluded from the present study. Regarding AD-related pathology, rare NFTs and  $\beta$ -amyloid deposits were found in iLBD (Braak stages 0-II; Thal phases 0-I); Braak stages I–III and Thal phases 0–3 were observed in PD; Braak stages 0–V and Thal phases 0–5 occurred in DLB. MA cases had not suffered from neurologic, psychiatric or metabolic diseases (including metabolic syndrome), and did not have abnormalities in the neuropathological examination excepting NFT pathology stages I–II and phases 0–2 of  $\beta$ -amyloid plaques.

## RNA EXTRACTION

Purification of RNA was carried out with RNeasy Lipid Tissue Mini Kit (Qiagen, Hilden, Germany) following the protocol provided by the manufacturer. During purification, samples were treated with RNase-free DNase Set (Qiagen) to avoid later amplification of genomic DNA. The concentration of each sample was obtained from A260 measurements with Nanodrop 1000. RNA integrity was tested using the Agilent 2100 BioAnalyzer (Agilent Technologies, Santa Clara, CA, USA). Values of RNA quality (RNA integrity number [RIN] values) were from 7 to 8.8 in the first series and from 6.2 to 8.2 in the second series.

## MICROARRAY ANALYSIS

Affymetrix microarray platform and the Genechip Human Gene 1.1 ST Array was used to analyze gene expression patterns on a whole-genome scale on a single array with probes covering several exons on the target genes. Starting material was 200 ng of total RNA from each sample. Sense ssDNA was generated from total RNA with the Ambion WT Expression Kit from Ambion

(Carlsbad, CA, USA), according to the manufacturer's instructions. Sense ssDNA was fragmented, labeled and hybridized to the arrays with the GeneChip WT Terminal Labeling and Hybridization Kit from Affymetrix. Chips were processed on an Affymetrix GeneTitan platform.

Preprocessing of raw data and statistical analyses were performed using Bioconductor packages in R programming environment. We read CEL files from Affymetrix arrays, corrected the background and summarized and normalized the data with the robust microarray method implemented in the Bioconductor Limma package (81). Then, fold change and SEs were assessed by fitting a linear model (using the *lmFit* function in Limma package) for each gene. Genes with empirical Bayes *t* test *P*-values at a level of 0.01 were selected. Multiple testing correction was performed by adjusting *P*-values for false discovery rate (FDR) using the Benjamini and Hochberg method (BH).

## GENE ENRICHMENT SCORE

The average expression values of different transcripts of the same gene were used for gene enrichment scores and weighted gene coexpression network analysis. Only genes in the upper 25% percentile of standard deviation of expression among samples were assessed. For probes mapping to multiple genes we fused all gene ids into one and that was considered a "gene" in the network analysis but not for functional annotation, gene ontology (GO) enrichment and protein-protein interactions (PPI) analysis, for which all individual ids were used.

An enrichment score per gene (5), which is a measure of specificity of a gene for a particular group, disease state in our study, was calculated relative to the rest of the groups tested. Briefly, the method is based on computing linear model coefficients contrasting all groups pair-wise. These coefficients represent a measure of difference between two groups in which more distant categories present higher coefficient values usually associated with lower *P*-values. The enrichment score of a gene in a group is the sum of its significant coefficients against all other groups.

The enrichment score for each of the 5114 genes under study was calculated after obtaining the linear models for microarray data with the LIMMA package (81) considering a linear coefficient statistically significant at uncorrected *P*-value lower than 0.01.

## WEIGHTED GENE COEXPRESSION NETWORK ANALYSIS

WGCNA was done in R using the WGCNA library (57). We first constructed a gene coexpression network based on pair-wise correlation of gene expression using all samples at the same time or independently for each disease condition. Not all network topologies fitted with the scale-free topology model (i.e., the iLBD network). Therefore, all subsequent analysis based on the coexpression network constructed with all samples used a soft-power threshold of 5. We identified modules of genes based on their topological overlap dissimilarity with their connection strengths in the weighted network (44, 66). Using the dynamic tree-pruning algorithm, 23 initial modules were obtained; genes not assigned to any module were labeled in gray. After merging all modules with highly correlated eigengenes (Pearson correlation

$\geq 0.8$ ), 13 final modules were obtained. Module eigengenes were correlated to LBD diagnostic. The *P*-values were obtained from a general multivariate lineal model including additional control variables (i.e., age, sex, RIN, PMI and batch).

## Gene enrichment analysis

GO enrichment analysis was performed using GOstats (27). Differentially expressed genes with uncorrected *P*-values  $< 0.01$  for each contrast were used for GO analysis. All genes belonging to a particular gene coexpression module were also used for independent GO analyses. *P*-values for categories were adjusted considering FDR using BH with the *p.adjust* function in R.

## PROTEIN-PROTEIN INTERACTION NETWORK

Assumed protein-protein interaction was obtained with BioGrid, latest release. Subnetworks of genes were obtained using the function-induced subgraph from the R library rTRM (73). Only nodes with evidence of physical interaction in humans were considered. Networks were analyzed and visualized using Cytoscape (87).

## REAL-TIME PCR

RT-qPCR assays were conducted in duplicate on 1000 ng of cDNA samples obtained from the retrotranscription reaction, diluted 1:20 in 384-well optical plates (Kisker Biotech, Steinfurt, GE) utilizing the ABI Prism 7900 HT Sequence Detection System (Applied Biosystems). Parallel amplification reactions were carried out using 20x TaqMan Gene Expression Assays and 2x TaqMan Universal PCR Master Mix (Applied Biosystems). TaqMan probes used in the study are shown in Supporting Information Table 1. The reactions were performed using the following parameters: 50°C for 2 minutes, 95°C for 10 minutes, 40 cycles at 95°C for 15 s and at 60°C for 1 minute. TaqMan PCR data were captured using the Sequence Detection Software (SDS version 2.2, Applied Biosystems). Subsequently, threshold cycle (CT) data for each sample were analyzed with the double delta CT ( $\Delta\Delta CT$ ) method. First, delta CT ( $\Delta CT$ ) values were calculated as the normalized CT values for each target gene in relation to the endogenous controls  $\beta$ -glucuronidase (GUS- $\beta$ ) and X-prolyl aminopeptidase P1 (XPNPEP1). These housekeeping genes were selected because they show no modifications in several neurodegenerative diseases in human postmortem brain tissue (4, 25). A similar pattern was observed using GUS- $\beta$  and XPNPEP1 for normalization (data not shown). The mean of GUS- $\beta$  and XPNPEP1 was used for correction and representation. Finally,  $\Delta\Delta CT$  values were obtained with the  $\Delta CT$  of each sample minus the mean  $\Delta CT$  of the population of control samples (calibrator samples). The fold-change was determined using the equation  $2^{-\Delta\Delta CT}$  (33).

## STATISTICAL ANALYSIS FOR RT-QPCR

The normality of distribution of the mean fold-change values obtained with RT-qPCR for every region and stage between controls and PD cases was analyzed with the Kolmogorov-Smirnov

test. The nonparametric Mann–Whitney test was performed to compare each group when the samples did not follow a normal distribution and the unpaired student's *T*-test was used for normal variables. Statistical analysis was performed with GraphPad Prism version 5.01 (La Jolla, CA, USA) and Statgraphics Statistical Analysis and Data Visualization Software version 5.1 (Warrenton, VA, USA). Differences between groups were considered statistically significant at *P*-values: \**P* < 0.05, \*\**P* < 0.01 and \*\*\**P* < 0.001. Additionally, BH-FDR adjusted *P*-values were obtained using the *p.adjust* function in R.

## RESULTS

### Differential gene expression and gene enrichment score in frontal cortex area 8 in iLBD, PD and DLB

We contrasted gene expression values of all possible pair-wise comparisons among all diagnostic groups. We selected differentially expressed genes or DEGs (see methods). We found most DEGs occurred between DLB and the rest of groups; in particular, most were genes downregulated in DLB compared to controls, followed by genes upregulated in DLB. Considering nominal *P*-values lower than 0.01, PD and iLBD showed fewer DEGs than DLB. Considering multiple-testing adjusted *P*-values < 0.05, only DLB cases produced differential expressed genes (DEG) genes comparable to controls, and no gene survived that threshold in iLBD and PD (Supporting Information Table 2).

We performed GO enrichment analysis focused on biological process categories for each group of DEGs independently in upregulated and downregulated genes (Supporting Information Table 3).

To summarize all pair-wise group comparison in one statistic, we calculated a gene enrichment score for each of the 5114 genes analyzed. The advantage of this approach is the possibility of highlighting genes that are differentially expressed in one group relative to all other groups. The score of a given gene summarizes differences in expression levels between comparisons among all four groups of samples. Positive or negative scores are associated with an increase or a reduction in expression, respectively, of each gene in a given group relative to the rest of the groups. We obtained 1914 genes with an enrichment score other than 0 in at least one of the groups. As revealed by clustering analysis, we found that DLB presented the highest number of genes with higher enrichment scores (Figure 1A). In agreement with the proportion of DEGs described above, gene scores in DLB were mostly negative (Figure 1A). The fifty top upregulated and top downregulated genes in DLB are listed in Supporting Information Table 4.

The main upregulated genes in frontal cortex in iLBD were associated with axonemal dynein complex assembly and taste receptors, whereas the main downregulated genes were linked to inflammation (Table 1).

The main upregulated genes in frontal cortex in DLB compared with controls were categorized into cellular development and DNA/RNA metabolism genes. The main downregulated genes in frontal cortex in DLB compared with controls were grouped into synapsis and neurotransmission, chaperone and protein folding, mitochondria and energy metabolism, purine metabolism and inflammation (Table 2).

### Weighted gene coexpression network analysis

Weighted gene coexpression network was constructed using the expression values of 5114 genes with variable expression among the 28 samples. Thirteen uncorrelated ( $r < 0.8$  gene modules were identified and labeled by colors and numbers (M1 to M13). The genes not assigned to any particular coexpression module were assigned to M0 or “gray” (Figure 1B).

We obtained the most representative pattern of gene expression across all samples for each one of these modules by calculating the eigengene (i.e., the first principal component). The eigengene of each module was then correlated with the LBD spectrum (iLBD, PD and DLB) obtaining an eigengene significance for each module (Figure 2A). Three modules, M4-lightcyan (157 genes), M6-tan (215 genes) and M10-darkred (23 genes) were negatively correlated with iLBD. M3-green (226 genes), M11-royalblue (23 genes) were positively and M10-darkred negatively, correlated to PD were negatively correlated with iLBD. M3-green (226 genes) and M11-royalblue (23 genes) were positively and M10-darkred negatively, correlated to PD. Three other modules, M3-green, M5-brown and M9-salmon, correlated significantly with DLB. M5-brown correlated negatively with DLB and contained 766 genes. M3-green and M9-salmon correlated positively with DLB and contained 226 and 51 genes, respectively (Figure 2B). None of our identified disease-correlated modules were also correlated with age, indicating that our disease associated modules are not significantly confounded by transcriptomic changes produced by normal ageing. Of note, one module, M7-midnightblue, was negatively correlated with age.

### Module characterization

Four strategies were used: (1) Identification of top highly connected genes (or hubs) in each module, (2) Assessment of overlaps with available published brain modules to correlate present LBD-associated modules to brain-related biological categories, (3) Identification of enriched GO among genes in each module and (4) Subdivision of each module into subnetworks based on available knowledge concerning physical PPI networks of human proteins.

### Top hub genes

MSN, UGT2B11, lysosomal protein transmembrane 5 (LAPTM5) gene was the top hub genes in the iLBD-associated modules M4-lightcyan, M10-darkred and M6-tan, respectively. MSN encodes for Moesin, a molecule that links cytoskeleton to membrane and which is a suggested phosphorylation target of LRRK2. UGT2B11 encodes a UDP-glucuronosyltransferase and LAPTM5 is a lysosomal gene recently identified as a hub node in the protein-interaction network obtained from DEGs in locus ceruleus in PD patients vs. healthy donors (18). Hub genes in M3-green and M11-royalblue, PD-associated modules, are genes with unknown function. ATP6V1B2 and ATPase, H<sup>+</sup> transporting, lysosomal 70 kDa, V1 subunit A (ATP6V1A) and stress-induced-phosphoprotein 1 (STIP1) were top hub genes for M5-brown and M9-salmon, respectively, linked to DLB modules. ATP6V1A encodes a component of vacuolar ATPase which mediates the acidification of intracellular organelles including endosomes, lysosomes, the trans-

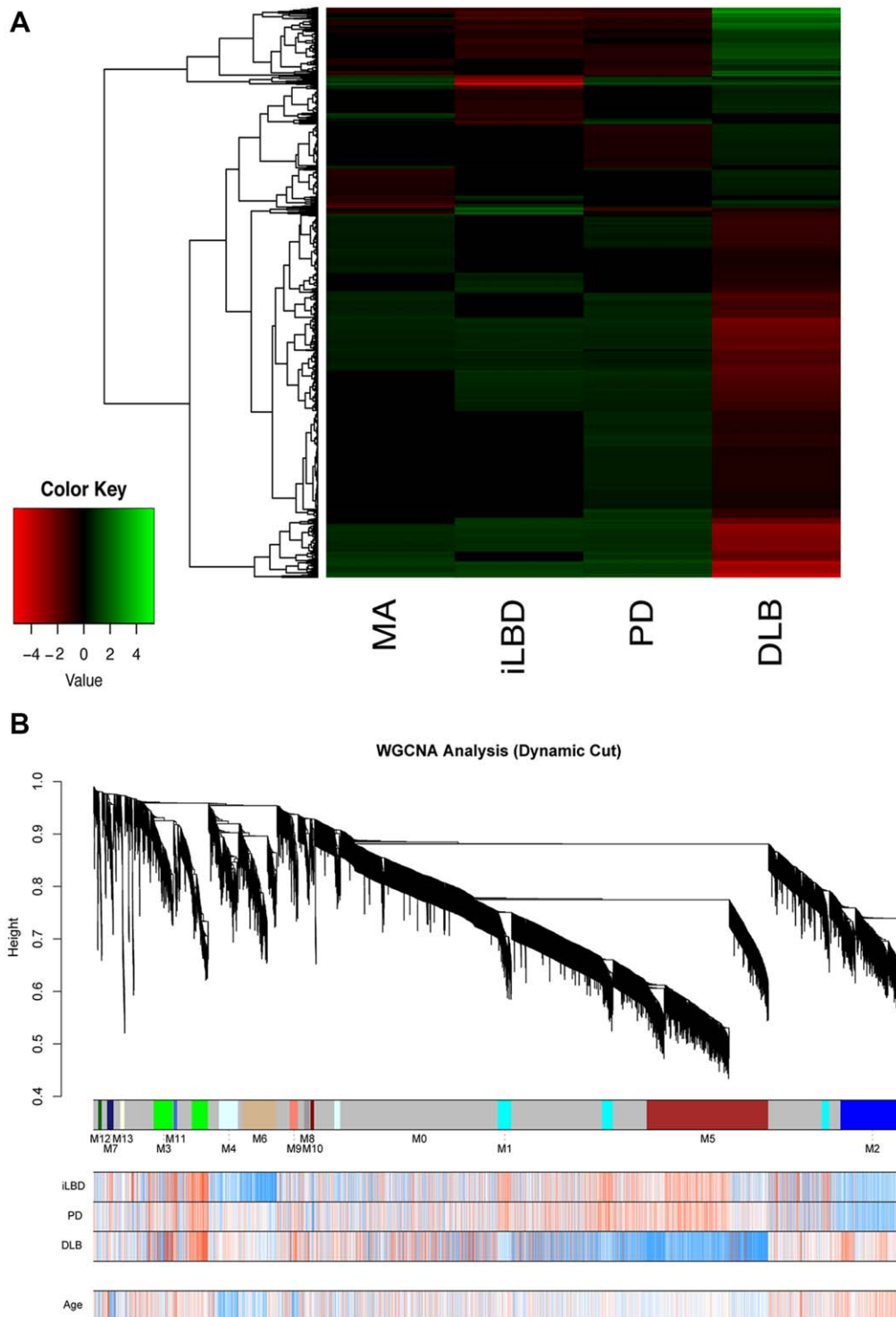


**Figure 1. A.** Heatmap representation of the enrichment scores of 1914 genes having at least one group of samples with enrichment scores other than 0. MA: middle-aged, iLBD: incidental Lewy body disease, PD: Parkinson disease, DLB: dementia with Lewy bodies.

**B.** Weighted gene coexpression network analysis of the frontal cortex transcriptome using 5114 gene expression values of 28 assessed samples identifies 13 gene modules. Modules are labeled by color

and number (M1 to M13). Genes not assigned to any particular coexpression modules were labeled M0 or gray. Dendrogram obtained by hierarchical clustering of genes based on their topological overlap is shown at the top. Bottom rows indicate the correlation value of each gene expression and the spectrum of LBD pathology. Blue to red indicates negative to positive correlation values. None of our identified modules correlated with age.

**Table 1.** Main deregulated gene clusters in frontal cortex in iLBD.

Cluster	Gene names	Count	Size	Odds Ratio	P-value	Deregulation
Adaptive immune response	C3AR1 C3 C1QC C1QB INPP5D PTPN6 ADA FCER1G CTSC TGFB1	10	58	12.64	0.00	Down
Antigen processing and presentation	SEC23A RAB3B PSMD8 PSMC2 PSMB2 ACTR1B LGMN RAB7A PSMB3 RAB3C DCTN6 AP1S1 PSMD12 DCTN2 DCTN3 PSMA5 AP2M1 PSMB6 PSMC4 PSMA3 PSMA4 DYNC111 KIF3A AP1M1	24	65	2.85	0.00	Down
Axonemal dynein complex assembly	LRRC6	1	2	353.08	0.01	Up
Cell activation involved in immune response	APBB1IP TYROBP VAMP8 ADA LCP1 FCER1G HLA-DMB TGFB1	8	52	10.72	0.00	Down
Detection of chemical stimulus involved in sensory perception of bitter taste	TAS2R4 TAS2R14	2	5	256.67	0.00	Up
Granulocyte activation	TYROBP FCER1G	2	7	21.94	0.01	Down
Innate immune response	CSF1R HLA-DPB1 AIF1 C3 TYROBP C1QC C1QB HLA-DPA1 TREM2 TRIM22 ITGB2 PTPN6 CYBB FCER1G RPS6KA1 VSIG4 TGFB1 CXCL16	18	277	4.53	0.00	Down
Lymphocyte activation involved in immune response	APBB1IP ADA LCP1 FCER1G HLA-DMB TGFB1	6	31	13.83	0.00	Down
Mononuclear cell proliferation	HLA-DPB1 AIF1 LST1 HLA-DPA1 INPP5D ITGB2 PTPN6 ADA HLA-DMB VSIG4 TGFB1	11	54	15.77	0.00	Down
Myeloid dendritic cell activation	TGFBR2 CD37 TGFB1	3	8	33.34	0.00	Down
Positive regulation of mast cell activation	VAMP8 FCER1G	2	7	21.94	0.01	Down
Regulation of B cell mediated immunity	C3 PTPN6 FCER1G TGFB1	4	8	56.34	0.00	Down
Regulation of immunoglobulin production	CD37 TGFB1	2	8	18.28	0.01	Down
T cell activation involved in immune response	APBB1IP LCP1 FCER1G HLA-DMB	4	13	25.01	0.00	Down

Golgi network and synaptic vesicles, thus enabling a plethora of functions such as zymogen activation, endocytosis, synaptic transmission and protein transport (12). STIP1 (HOP) is implicated in assisting the function of chaperone protein interaction with HSP70 and HSP90 (72) (Supporting Information Table 5).

### Overlap of modules with reported brain-related categories: specific cell populations and particular diseases

Module M6-tan and M4-lightcyan were highly enriched in markers of microglia (15). M5-brown and M9-salmon DLB-associated modules were found enriched in neuronal and microglial markers (24, 58) (Figure 3, Supporting Information Table 6). Other modules identified in our study, but not correlated with LBD, showed enrichment in particular cell types. For instance, M2-blue module was enriched in oligodendrocyte markers whereas M1-cyan and M7-midnightblue were enriched in neuronal and glial cell markers. These observations support the biological consistency of our network and the robustness of the method to build similar transcriptional modules using different sources of data.

M6-tan modules presented enrichment in genes that was also deregulated at early stages of AD (75). Moreover, module M5-brown showed overlap with deregulated gene sets and modules reported in AD (6, 60). These confluences suggest commonalities involving multiple processes in these neurodegenerative diseases. In fact, DLB is largely associated with AD-related pathology, and DLB cases in the present series had associated AD pathology.

### Identification of enriched GO among genes in each module

We also attempted to relate genes in modules to particular GO. Consistent with the microglial nature of this module, genes in M6-tan were highly enriched in GO categories related to immune system and inflammation. Similarly, M4-lightcyan was also enriched in categories related to inflammatory defence response. Module M5-brown showed highly significant enrichment in GO categories related to synaptic transmission and energy metabolism, among others. Genes in M9-salmon module presented a highly significant enrichment in GO categories related to protein folding and heat-shock chaperone activity. Interestingly, the age associated M7-midnightblue module was enriched in GO categories such as hormone response, oxidative stress and learning, among others. Supporting Information Table 7 shows the full list of categories in modules 3, 5, 6, 9 and 11. Only few genes composed M11-royalblue and M10-darkred for proper GO analysis, but those modules contained taste 2 receptor members (TAS2R10, TAS2R4, TAS2R50) and nine olfactory receptors, respectively.

### Putative subnetworks of protein-protein interactions

We intersected genes from each coexpression module with PPI databases to identify putative subnetworks with biological relevance within modules. Genes in M6-tan, M4-lightcyan, M5-brown and M9-salmon each produced notable PPI subnetworks composed of 44, 51, 302 and 21 genes, respectively (representing 25.7%,

**Table 2.** Main deregulated gene clusters in frontal cortex in DLB.

Cluster	Gene names	Count	Size	Odds ratio	P-value	Deregulation
Antigen processing and presentation	SEC23A RAB3B PSMB8 PSMC2 PSMB2 ACTR1B LGMN RAB7A PSMB3 RAB3C DCTN6 AP1S1 PSMD12 DCTN2 DCTN3 PSMA5 AP2M1 PSMB6 PSMC4 PSMA3 PSMA4 DYNC111 KIF3A AP1M1	24	65	2.85	0.00	Down
Antigen processing and presentation of exogenous peptide antigen via MHC class II	SEC23A ACTR1B LGMN RAB7A DCTN6 AP1S1 DCTN2 DCTN3 AP2M1 DYNC111 KIF3A AP1M1	12	29	3.40	0.00	Down
Apoptotic mitochondrial changes	SLC25A4 YWHAZ MLLT11 DNMI1L PARK2 FAM162A YWHAB MAPK9 BLOC1S2 YWHAG GSK3B GGCT OPA1 PIM2	14	40	2.60	0.01	Down
ATP hydrolysis coupled proton transport	ATP6V1F ATP5B ATP6V1E1 ATP6AP1 ATP6V1B2 ATP5G1 ATP6V0D1 ATP6V1C1 ATP6V1A ATP1A1 ATP6V0A1 ATP1A3 ATP6V1H ATP5A1 COX8A NDUFB5 ATP5B OLA1 NDUFA5 ATP6V1B2 ATP5G1 ENTPD5 DLD HTR2A DNMI1L PRKAG1 ATP6V1A CYCS ENO2 NDUFA9 UQCRC1 PGK1 UQCRC2 ATP6V0A1 BPGM HK1 NDUFS3 GBAS NDUFS4 NDUFV2 ATP5H PPP2R5D NDUFAB1 ATP5A1	14	17	22.66	0.00	Down
ATP metabolic process	AKR1C2 PRXG GJA1 NUPR1 P2RX7 FGF17 TYK2 TOB2 HDAC4 MSX1 RXRA IKBKB FLCN PTCH1 YAP1 CD151 NACC2 LRP2 ID4 TNS3 KAT2A CDC14A GPER1 FOXO1 FOXC1 RELA EPS8	30	77	3.13	0.00	Down
Cell proliferation	IDH3G PNPO MDH2 PDHB IDH3B ACLY RFK AASDHPPT ENTPD5 DLD HTR2A DLAT PRKAG1 ENO2 NMINAT2 MDH1 NDUFA9 SLC25A32 PDP1 PGK1 ELOVL6 ELOVL4 BPGM FAR2 HK1 PTS PDK3 ACSL4 SUCLA2 KCNAB2 PPP2R5D MVK MAT2B	27	536	2.04	0.00	Up
Coenzyme metabolic process	EYA2 RBM14 HDAC4 FLCN NACC2 KAT2A DOT1L PRELP KLF15 NPPT1 AKR1C2 PRXG LRP4 GJA1 WWC3 SLC5A3 NUPR1 P2RX7 FGF17 EYA2 TYK2 AK4 CPQ TOB2 HDAC4 CAPN2 ADGRV1 MSX1 MRAS PPP2R1B RXRA IKBKB SASH1 ANKRD11 CDC42EP4 ZIC2 FLCN PTCH1 PCID2 MT1G YAP1 S100A1 ID3 CA2 DNAJB6 GNA12 ROCK1 LRP2 RAMP1 PPP1R13L SPR FRYL ARAP1 ID4 HIF3A SRGAP1 SLC39A12 VCAN TNS3 KAT2A CDC14A GPER1 FOXO1 FOXC1 MAN2A1 EHD2 P116 RELA EPS8	33	113	2.01	0.00	Down
Covalent chromatin modification	EYA2 RBM14 HDAC4 FLCN NACC2 KAT2A DOT1L	7	80	3.41	0.01	Up
Developmental process	PRELP KLF15 NPPT1 AKR1C2 PRXG LRP4 GJA1 WWC3 SLC5A3 NUPR1 P2RX7 FGF17 EYA2 TYK2 AK4 CPQ TOB2 HDAC4 CAPN2 ADGRV1 MSX1 MRAS PPP2R1B RXRA IKBKB SASH1 ANKRD11 CDC42EP4 ZIC2 FLCN PTCH1 PCID2 MT1G YAP1 S100A1 ID3 CA2 DNAJB6 GNA12 ROCK1 LRP2 RAMP1 PPP1R13L SPR FRYL ARAP1 ID4 HIF3A SRGAP1 SLC39A12 VCAN TNS3 KAT2A CDC14A GPER1 FOXO1 FOXC1 MAN2A1 EHD2 P116 RELA EPS8	62	1671	1.65	0.00	Up
Electron transport chain	COX8A NDUFB5 ATP5B NDUFA5 ATP5G1 ALDH5A1 DLD CYCS NDUFA9 UQCRC1 SLC25A14 UQCRCF51 UQCRC2 SLC25A12 NDUFS3 NDUFS4 NDUFV2 ATP5H NDUFAB1 ATP5A1	20	43	4.23	0.00	Down
Exocytosis	VPS33B TUBA4A SNX4 CDK5 NAPA RAB3B RPH3A PLCB1 PFN2 SYT5 ATP6AP1 PAK1 CHP1 SCAMP1 SCFD2 RAB7A RAB3C RASGRP1 SCAMP5 NSF SNAP25 HABP4 RAB3A VPS33A KIT VAMP1 PPIA VSNL1 STXBP1 RAB27B VPS4B SYT13 CRHBP VAMP2 RALB BLOC1S6 SYT16 CDK5R2 SYT1 DOC2A ARHGAP44 PPP3CB GOT1 MDH2 RBP4 SLC35B4 ENO2 MDH1 PRKACA PGK1 G6PC3 BPGM SLC25A12 GOT2	42	160	1.74	0.00	Down
Gluconeogenesis	GOT1 MDH2 RBP4 SLC35B4 ENO2 MDH1 PRKACA PGK1 G6PC3 BPGM SLC25A12 GOT2	12	31	3.04	0.00	Down
Histone modification	EYA2 RBM14 HDAC4 FLCN NACC2 KAT2A DOT1L	7	80	3.41	0.01	Up
Innate immune response activating cell surface receptor signaling pathway	PAK1 PSMB8 PSMC2 PSMB2 PSMB3 PRKACA PSMD12 PSMA5 PSMB6 UBE2N PSMC4 PSMA3 PSMA4 TAB3 PPP3CB	15	44	2.50	0.01	Down

**Table 2. Continued.**

Cluster	Gene names	Count	Size	Odds ratio	P-value	Deregulation
miRNA metabolic process	PNPT1, RELA	2	4	34.69	0.00	Up
Mitochondrial electron transport, NADH to ubiquinone	NDUFB5, NDUFA5, DLD, NDUFA9, NDUFS3, NDUFS4, NDUFV2, NDUFAB1	8	16	4.81	0.00	Down
Mitochondrial translation	MRPL15, MRPL30, MRPL37, HARS, MTFMT, LRPPRC, CHCHD1, MRPL45, MPV17L2, MRPS21, MRPL42	11	27	3.31	0.00	Down
Mitochondrial transport	TOMM20, VPS11, MPC2, ATP5B, YWHAZ, PSMD8, ATP5G1, TIMM17A, HAX1, PARK2, TOMM34, TOMM70A, TOMM22, SLC25A32, BAG4, NRG1, SLC25A14, YWHAB, MAPK9, UGCG, BLOC1S2, YWHAG, DNAJC19, SLC25A12, MTX3, GSK3B, MICU1, KIF1BP, ATP5H, ATP5A1	30	104	1.97	0.00	Down
mRNA polyadenylation	PNPT1, PAPOLA	2	4	34.69	0.00	Up
NADH metabolic process	IDH3G, MDH2, IDH3B, ENO2, MDH1, PGK1, HK1, PFP2R5D	8	18	3.85	0.01	Down
Neuron-neuron synaptic transmission	CDK5, NAPA, RAB3B, PAK1, CHRN2, CAMK4, CACNB4, GABRA1, HTR2A, GRIN2A, SLC6A1, PARK2, PRKACA, GABRG2, STXBP1, GLRA2, MEF2C, GRIA3, CRHRP, GRIN3A, SYT1, DNMI1, PNKD	23	80	1.95	0.01	Down
Neurotransmitter transport	SLC32A1, CDK5, GAD1, SV2C, GAD2, NAPA, RAB3B, RPH3A, PFN2, SYT5, PAK1, ALDH5A1, SV2A, NRXN3, PPT1, SLC6A1, SLC6A17, RAB3C, PARK2, SNAP25, RAB3A, ATP2A2, STXBP1, SLC38A1, SYT13, MEF2C, VAMP2, BLOC1S6, SYT16, SYT1, DOC2A, SV2B, ICA1	33	112	2.04	0.00	Down
Nucleobase-containing compound metabolic process	KLF15, PNPT1, ZNF471, AHNAK, GJA1, PAN2, WWC3, NUPR1, P2RX7, EYA2, RBM14, AK4, HDAC4, SAFB2, MSX1, RBMS2, RXRA, IKBKB, TRIM52, ZIC2, FLCN, RAD52, IFI27, PTCH1, PCID2, YAP1, S100A1, ID3, SNRNP48, ZFHX2, DNAJB6, NACC2, CRY1, RAMP1, PPP1R13L, FRYL, ID4, HIF3A, PAPOLA, KAT2A, RFX2, ZNF347, GPER1, TCP10L, FOXO1, POLN, TOP3B, FOXC1, RELA, GABPB2, DOT1L, RBM4B, MICAL3	53	1235	1.94	0.00	Up
Phagosome maturation	ATP6V1F, ATP6V1E1, ATP6V1B2, ATP6V0D1, ATP6V1C1, RAB7A, ATP6V1A, ATP6V0A1, ATP6V1H, ATP6V1D	10	18	6.03	0.00	Down
Proteasome-mediated ubiquitin-dependent protein catabolic process	ERLEC1, USP5, KCTD13, PSMD8, PSMD2, PSMB2, USP11, PSMB3, PARK2, USP10, UBXN11, FBXO9, PRICKLE1, FBXL2, PSMD12, PLK2, RNF185, PSMA5, PSMB6, PSMA4, UCHL1, UBE2W, PSMA3, GSK3B, PSMA4, GLMN, BBS7, RNF14, RNF4, NEDD4L	30	99	2.12	0.00	Down
Protein K11-linked ubiquitination	UBE2E2, PARK2, UBE2W, UBE2T, RNF4	5	7	11.99	0.00	Down
Protein K6-linked ubiquitination	PARK2, UBE2T, RNF4	3	3	Inf	0.01	Down
Protein monoubiquitination	PARK2, FBXL2, UBE2W, TRIM37, RNF2, UBE2T	6	11	5.76	0.01	Down
Protein ubiquitination involved in ubiquitin-dependent protein catabolic process	PSMD8, PSMD2, PSMB2, PSMB3, PARK2, PSMD12, PSMA5, PSMB6, PSMA4, PSMA3, PSMA4, RNF14, NEDD4L	13	37	2.61	0.01	Down
Proton transport	COX8A, ATP6V1F, ATP5B, ATP6V1E1, SLC9A7, ATP6AP1, ATP6V1B2, ATP5G1, ATP6V0D1, CHP1, ATP6V1C1, ATP6V1A, SLC9A6, COX7A2, UQCRC1, SLC25A14, ATP1A1, UQCRCF1, SLC2A13, ATP6V0A1, ATP1A3, ATP6V1H, ATP5H, SLC9B2, ATP6V1D, ATP5A1	26	59	3.86	0.00	Down
Purine nucleoside metabolic process	DGUOK, COX8A, NDUFB5, ATP5B, PRPS1, OLA1, MPP1, NDUFA5, ATP6V1B2, HPRT1, ATP5G1, ACLY, ENTPD5, DLD, HTR2A, DNMI1, PRKAG1, ATP6V1A, CYCS, ENO2, NDUFA9, UQCRC1, DLG3, PGK1	37	111	2.46	0.00	Down



Table 2. Continued.

Cluster	Gene names	Count	Size	Odds ratio	P-value	Deregulation
Regulation of cell cycle	UQCRC2 ATP6V0A1 BPGM HK1 NDUFS3 GBAS NDUFS4 NDUFV2 ATP5H PPP2R5D NDUFAB1 MAT2B ATP5A1 PNPT1 NUPR1 RBM14 KLHL21 MSX1 FLCN PTCH1 PCID2 ID3 NACC2 CRY1 CENPJ CDC14A GPER1 FOXC1 CTDSP2 CAB39L DOT1L KLF15 ZNF471 AHNAK GJA1 WWC3 NUPR1 P2RX7 EYA2 RBM14 TOB2 HDAC4 SAFB2 MSX1 RXRA IKBKB TRIM52 ZIC2 FLCN IFI27 PTCH1 PCID2 YAP1 S100A1 ID3 ZFH2 DNAJB6 NACC2 CRY1 PPP1R13L FRYL ID4 HIF3A PAPOLA KAT2A RFX2 ZNF347 GPER1 TCP10L FOXO1 FOXC1 RELA GABPB2 DOT1L RBM4B MICAL3 KLF15 ZNF471 GJA1 WWC3 NUPR1 MARCH8 EYA2 RBM14 HDAC4 SAFB2 MSX1 RXRA IKBKB TRIM52 ZIC2 FLCN IFI27 PTCH1 PCID2 YAP1 S100A1 ID3 ZFH2 DNAJB6 NACC2 CRY1 RAMP1 PPP1R13L FRYL ID4 HIF3A KAT2A RFX2 ZNF347 GPER1 TCP10L FOXO1 FOXC1 RELA GABPB2 DOT1L RBM4B MICAL3	18	259	2.82	0.00	Up
Regulation of gene expression	VPS11 BECN1 YWHAZ PSMD8 MLLT11 DDHD2 DNM1L HAX1 PARK2 FAM162A BAG4 NRG1 YWHAB UGCG LRPPRC YWHAG HK1 GSK3B OPA1 MPV17L2	45	908	2.24	0.00	Up
Regulation of macromolecule biosynthetic process	PSMD8 PSMD2 PSMB2 PSMB3 PIN1 PSMD12 PSMA5 PSMB6 UBE2N PSMC4 PSMA3 DYNC1L11 LCMT1 PSMA4 SLC32A1 CDK5 GAD1 NCALD CALB1 GAD2 NAPA RAB3B GNG3 RPH3A PLCB1 PFN2 SYT5 PAK1 KCND2 ASIC2 ALDH5A1 GABRA3 HCN1 NRXN3 LRR1M1 CHRN2 CAMK4 CACNB4 PPT1 GABRA1 ARHGEF9 HTR2A GRIN2A SLC6A1 KCNAB1 RAB3C PARK2 CACNG3 SEZ6 PRKACA SST NSF SNAP25 GABRA4 GABRG2 KCNC2 RAB3A LRRTM2 KIT PLK2 DLG3 GRIN2B RASGRF1 HTR4 ATP2A2 GABRA5 STXBP1 SNCB SLC38A1 AP2M1 SYT13 GLRA2 MEF2C GRIA3 CRHBP VAMP2 YWHAG GRIN3A FGF12 KCNQ5 NETO1 NCDN BLOC1S6 SYT16 CACNB1 SYT1 DOC2A CHRM4 GABRB3 KCNH7 GNAL KCNAB2 GABBR2 CACNG2 DNM1 PCDH8 PANX1 AKAP5 PNKD PPP3CB SYP FGF14	43	863	2.23	0.00	Up
Regulation of mitochondrion organization	CDK5 RAB3B CHRN2 PARK2 CRHBP PNKD KLF15 AKR1C2 PRX LRP4 GJA1 NUPR1 P2RX7 EYA2 CPQ HDAC4 MSX1 RXRA IKBKB ZIC2 PTCH1 YAP1 ID3 CA2 ROCK1 PPP1R13L KAT2A FOXC1 MAN2A1 PI16 RELA KLF15 WWC3 RBM14 HDAC4 MSX1 RXRA IKBKB FLCN IFI27 PTCH1 YAP1 S100A1 ID3 NACC2 CRY1 PPP1R13L ID4 HIF3A PAPOLA KAT2A RFX2 GPER1 TCP10L FOXO1 FOXC1 RELA GABPB2 MICAL3 KLF15 ZNF471 WWC3 NUPR1 EYA2 RBM14 HDAC4 SAFB2 MSX1 RXRA IKBKB TRIM52 ZIC2 FLCN IFI27 PTCH1 PCID2 YAP1 S100A1 ID3 ZFH2 DNAJB6 NACC2 CRY1 PPP1R13L FRYL ID4 HIF3A PAPOLA KAT2A RFX2 ZNF347 GPER1 TCP10L FOXO1 FOXC1 RELA GABPB2 DOT1L MICAL3	20	66	2.10	0.01	Down
Regulation of ubiquitin-protein transferase activity		14	40	2.60	0.01	Down
Synaptic transmission		88	390	1.44	0.00	Down
Synaptic transmission, dopaminergic		6	12	4.80	0.01	Down
Tissue development		25	493	2.04	0.00	Up
Transcription from RNA polymerase II promoter		28	461	2.57	0.00	Up
Transcription, DNA-templated		40	785	2.24	0.00	Up

Table 2. Continued.

Cluster	Gene names	Count	Size	Odds ratio	P-value	Deregulation
Ubiquitin-dependent protein catabolic process	ERLEC1 USP5 KCTD13 PSMD8 PSMC2 PSMB2 USPT1 PSMB3 PARK2	37	123	2.11	0.00	Down
	NDVIP1 USP10 UBXN11 FBXO9 PRICKLE1 FBXL2 PSMD12 PLK2					
	RLIM RNF185 VPS25 PSMA5 VPS4B PSMB6 UBE2N PSMC4 COPS3					
	UCHL1 UBE2W PSMA3 GSK3B PSMA4 GLMN BBS7 RNF14 RNF4 UCHL5 NEDD4L					
Vesicle docking	VPS33B RAB3B SCFD2 RAB3C NSF SNAP25 RAB3A VPS33A STXBP1	13	28	4.19	0.00	Down
	RAB27B RALB STX12 BLOC1S6					
Vesicle organization	VPS11 VPS33B SNX4 SEC23A COPG1 NSG1 RAB7A SNAP25 COPZ1	24	79	2.12	0.00	Down
	RAB3A VAMP1 PRKCI PTPRN STXBP1 VPS4B SNX10 BLOC1S2					
	VAMP2 STX12 VTA1 BLOC1S6 HMP19 AP1M1 SYP					

35.4%, 47.2% and 45.7% of the genes in the module listed in the PPI database). Regarding M6-tan module PPI subnetwork, spleen tyrosine kinase (encoded by SYK) appeared with 16 interacting partners as the nucleating gene with highest degree (Figure 4A). M4-lightcyan included a subnetwork with CDK2, MSN and TP53 as top degree nodes (Figure 4B). Heat-shock related proteins encoded by genes STIP1, heat shock 70 kDa protein 5 (glucose-regulated protein, 78 kDa) (HSPA5), AHSA1 and heat shock 70 kDa protein 1A (HSPA1A) were the highest connected nodes in the M9-salmon PPI subnetwork (Figure 4C). M5-brown module contained a large PPI subnetwork with several nodes including proteins encoded by tyrosine 3-monooxygenase/tryptophan 5-monooxygenase activation protein, beta polypeptide (YWHAB), TP1A, glycogen synthase kinase 3 beta (GSK3B), proteasome (prosome, macropain) subunit, alpha type, 3 (PSMA3) and SNCA, among others (Figure 4D).

These results allow for better characterization of selected LBD-associated modules. M5-brown globally downregulated in DLB and enriched in neuronal markers and in genes mostly related to synaptic transmission and energy metabolism presented ATP6V1B2 and YWHAB as top hub genes in the transcriptomic and PPI networks, respectively. Other highly connected molecules were GSK3B, PSMA3, ATP6V0D1, triosephosphate isomerase 1 (TPI1), ATP6V1A and SNCA. Finally, an M9-salmon module, globally upregulated in DLB, was characterized by significant enrichment in genes involved in heat-shock protein folding and microglial markers, and was nuclearized around the hub gene STIP1 in both transcriptomic and PPI networks. Other highly interacting proteins were encoded by DnaJ (Hsp40) homolog, subfamily A, member 1 (DNAJA1), DnaJ (Hsp40) homolog, subfamily B, member 1 (DNAJB1), DnaJ (Hsp40) homolog, subfamily B, member 4 (DNAJB4), HSPA5, HSAPA6, AHSA1 and HSPA1A.

**RT-qPCR validation**

LAPTM5, a top gene in M6, was found not to be deregulated in iLBD, PD and DLB. ATP6V1A, one of the top genes in M5, was downregulated in DLB ( $1.03 \pm 0.25$  vs.  $0.57 \pm 0.52$ ,  $P = 0.007$ ). The expression of STIP1, one top gene in M9, was not significantly altered in DLB but only in a subset of rpDLB (see later) and in PD ( $1.03 \pm 0.28$  vs.  $1.75 \pm 0.70$ ,  $P = 0.006$ ); however, mRNA expression of DNAJA1 and DNAJB1, other top genes in the same module, was significantly increased in DLB (see later). SYK, the principal PPI in M6 was not deregulated in iLBD, PD and DLB (MA:  $1.06 \pm 0.51$ , iLBD:  $0.81 \pm 0.58$ , PD:  $1.02 \pm 0.38$ , DLB:  $1.47 \pm 0.93$ ).

TPI1, a PPI member of module 5, was upregulated in PD ( $1.02 \pm 0.20$  vs.  $1.29 \pm 0.14$ ,  $P = 0.004$ ). No significant modifications in the expression mRNA levels were observed for selected PPI members of M5 and M9 modules in DLB. However, several members were deregulated in a subpopulation of DLB cases characterized by their rapid course and classified as rpDLB. Regarding M5, upregulated genes in rpDLB were GSK3B ( $1.03 \pm 0.22$  vs.  $1.62 \pm 0.88$ ,  $P = 0.046$ ), whereas PSMA3 ( $1.01 \pm 0.15$  vs.  $0.57 \pm 0.05$ ,  $P = 0.000$ ) and YWHAB ( $1.01 \pm 0.15$  vs.  $0.69 \pm 0.22$ ,  $P = 0.007$ ) were downregulated. Genes representative of PPI in M9 were upregulated in rpDLB: HSPA1A ( $1.01 \pm 0.40$  vs.  $3.10 \pm 2.00$ ,  $P = 0.007$ ), HSPA5 ( $1.06 \pm 0.38$  vs.  $2.14 \pm 0.83$ ,  $P = 0.003$ ) and STIP1 ( $1.03 \pm 0.28$  vs.  $2.07 \pm 1.10$ ,  $P = 0.009$ ).

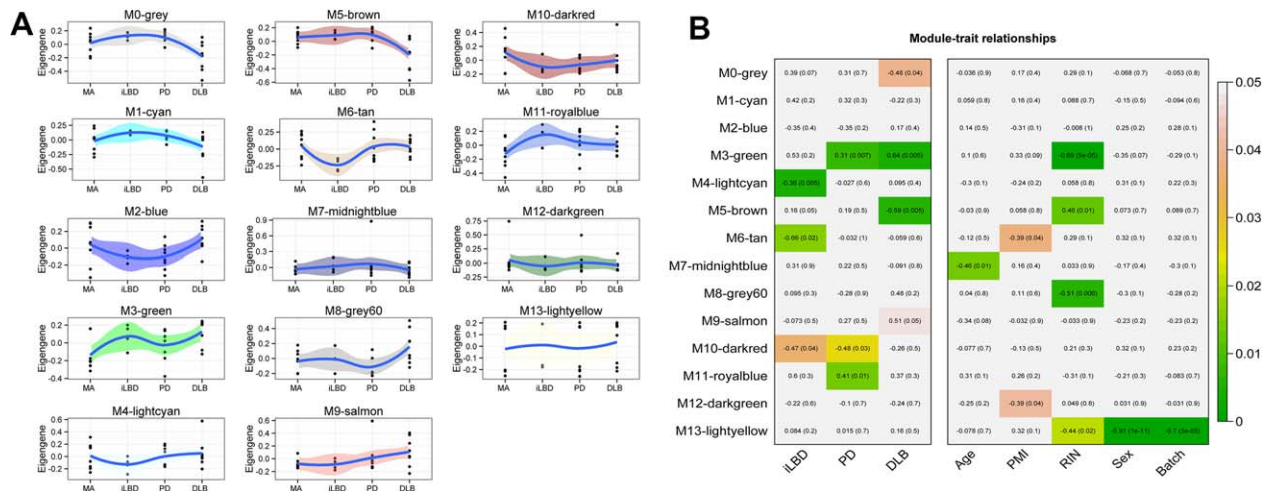


**Figure 2. A.** Module eigengenes for each module by LB spectrum. **B.** Correlation values (univariate) and *P*-values for the relationship between each module eigengene and each LBD stage compared separately with MA or various control variables. *P*-values for LBD

Abnormal regulation of the dynein cluster was assessed by RT-qPCR in LBDs with particular attention on iLBD. TASRs were assessed in iLBD, PD and DLB. Three biological functions, RNA/DNA metabolism, chaperone and protein folding, and synaptic neurotransmission, were selected for validation in DLB. We extracted those pathways and clusters from each of those categories that appeared in the corresponding module and disease in which the category appeared as significantly enriched.

Regarding dyneins, dynein axonemal assembly factor 1 (DNAAF1), dynein axonemal heavy chain 11 (DNAH11), dynein axonemal heavy chain 2 (DNAH2), dynein axonemal heavy chain 7 (DNAH7) and dynein axonemal intermediate chain 1 (DNAI1), but not dynein axonemal heavy chain 5 (DNAH5) and dynein axonemal heavy chain 9 (DNAH9), were significantly upregulated in iLBD when compared with MA. Interestingly, upregulation also occurred in PD and DLB. Taste receptor TAS2R5 and TAS2R13 were upregulated and downregulated, respectively, in iLBD; TAS2R10 upregulated in PD, and TAS2R4, TAS2R5, TAS2R14, TAS2R10 and TAS2R13 significantly upregulated in DLB (Table 3).

Moving on to iLBD, expression of allograft inflammatory factor 1 (AIF1) (which encodes IBA-1) was downregulated, as predicted, in frontal cortex (control:  $1.07 \pm 0.41$ , iLBD:  $0.57 \pm 0.20$ ,  $P = 0.018$ ). Focusing on DLB, polyribonucleotide nucleotidyltransferase 1 (PNPT1), poly(A) polymerase alpha (PAPOLA), RELA (proto-oncogene, NF- $\kappa$ B subunit) and DOT1 like histone lysine methyltransferase (DOT1L) mRNAs, all of them involved in RNA/DNA metabolism, but not lysine acetyltransferase 2A (KAT2A), were significantly upregulated in DLB (Table 4). Importantly, PNPT1 and RELA were upregulated in iLBD, and KAT2A was added in PD (Table 4).

Chaperone members DNAJA1, DnaJ (Hsp40) homolog, subfamily A, member 4 (DNAJA4), DNAJB1, heat shock 70 kDa protein 4 (HSPA4), heat shock 70 kDa protein 6 (HSP70B) (HSPA6) and heat shock 60 kDa protein 1 (chaperonin) (HSPD1), but not DNAJB4, HSPA1A, HSPA5 and MOB family member 4, phocin

(HSPE1), were significantly upregulated in frontal cortex area 8 in DLB when compared with MA (Table 4). No modification in the expression of these genes was found in iLBD, but DNAJA1, HSPA4 and HSPA5 mRNA expression was significantly increased in PD (Tables 3 and 4).

Finally, neurotransmission-related components gamma-aminobutyric acid B receptor, 2 (GABBR2), gamma-aminobutyric acid A receptor, alpha 1 (GABRA1), glutamate decarboxylase 1 (brain, 67 kDa) (GAD1) and synaptic proteins neuropilin and tollid-like 1 (NETO1), as well as synaptophysin (SYP) mRNAs, were found to be significantly downregulated in DLB when compared with MA. The expression of glutamate receptor, ionotropic-methyl D-aspartate 2A (GRIN2A) and glutamate receptor, ionotropic-methyl D-aspartate 2B (GRIN2B), and synaptic proteins member RAS oncogene family (RAB3A), Rabphilin 3A homolog (mouse) (RPH3A), synaptosomal-associated protein, 25 kDa (SNAP25), syntaxin binding protein 1 (STXBPI), synaptotagmin I (SYT1), synaptotagmin XIII (SYT13) and Synaptotagmin XVI (SYT16), was not altered in DLB (Table 4).

## DISCUSSION

This study presents the first transcriptome analysis of the frontal cortex integrating the whole spectrum of LBDs. In addition to performing a traditional gene-based differential expression analysis we considered a system biology approach based on coexpression networks. In particular, we applied WGNCA which allows the identification of modules of genes that are coexpressed across samples. These modules have to be interpreted with the understanding that such coexpression reflects a common biological function (e.g., from biochemical pathways to cell type defining signatures). We have identified some modules that correlate with LBDs. A proportion of genes included in those modules are also differentially expressed in a traditional gene-based comparative approach using the same microarray data and using independent case series for RT-qPCR quantification and validation. The present study has also

### Brain lists

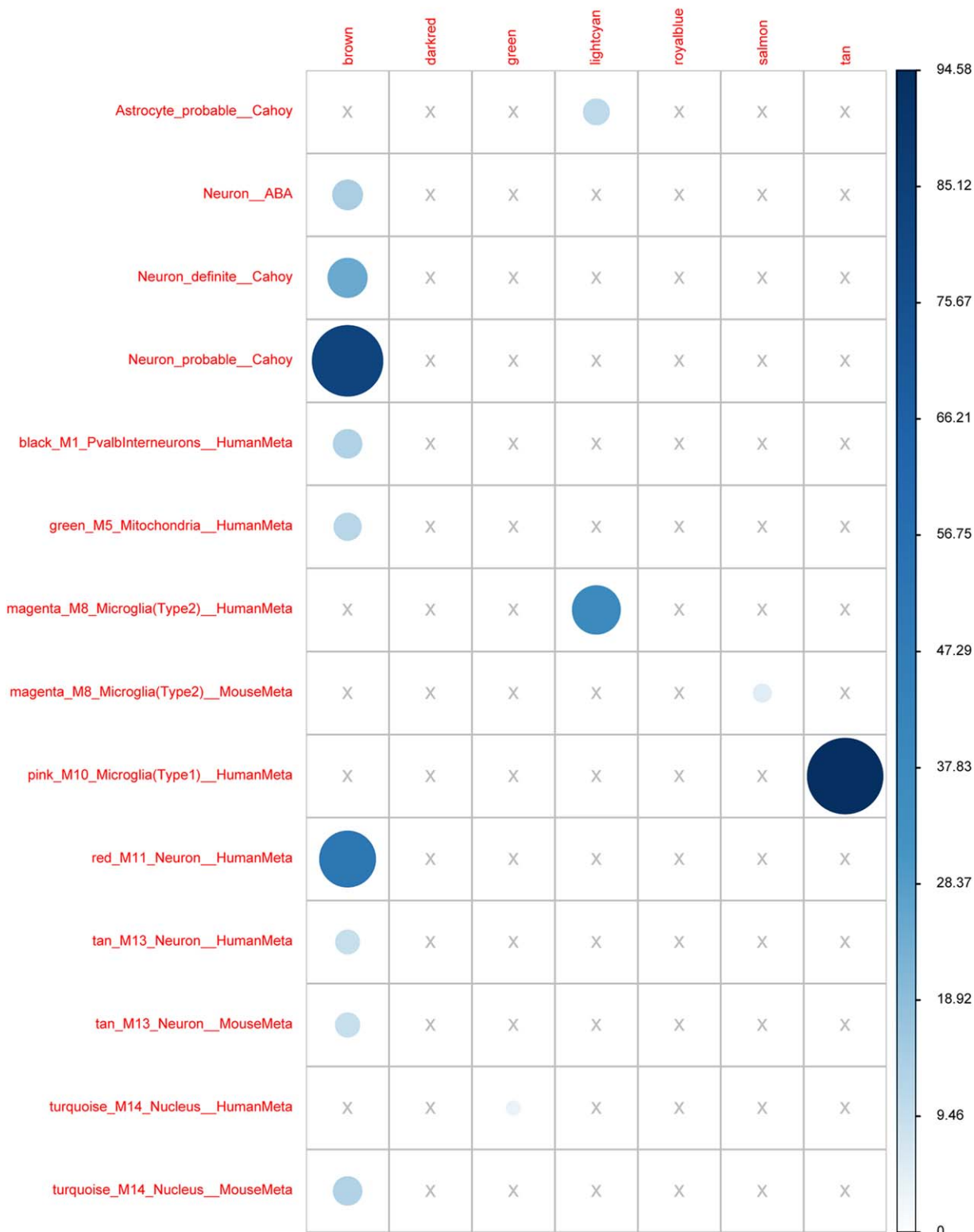


**Figure 3.** Enrichment score (-log<sub>10</sub> P-value) of genes in selected modules in previously published brain gene sets associated with cell types or brain regions. Module-brown (M6) is enriched in neuronal genes; module-tan (M5) is enriched in microglial genes; module-salmon (M6) has non-specific enrichment.

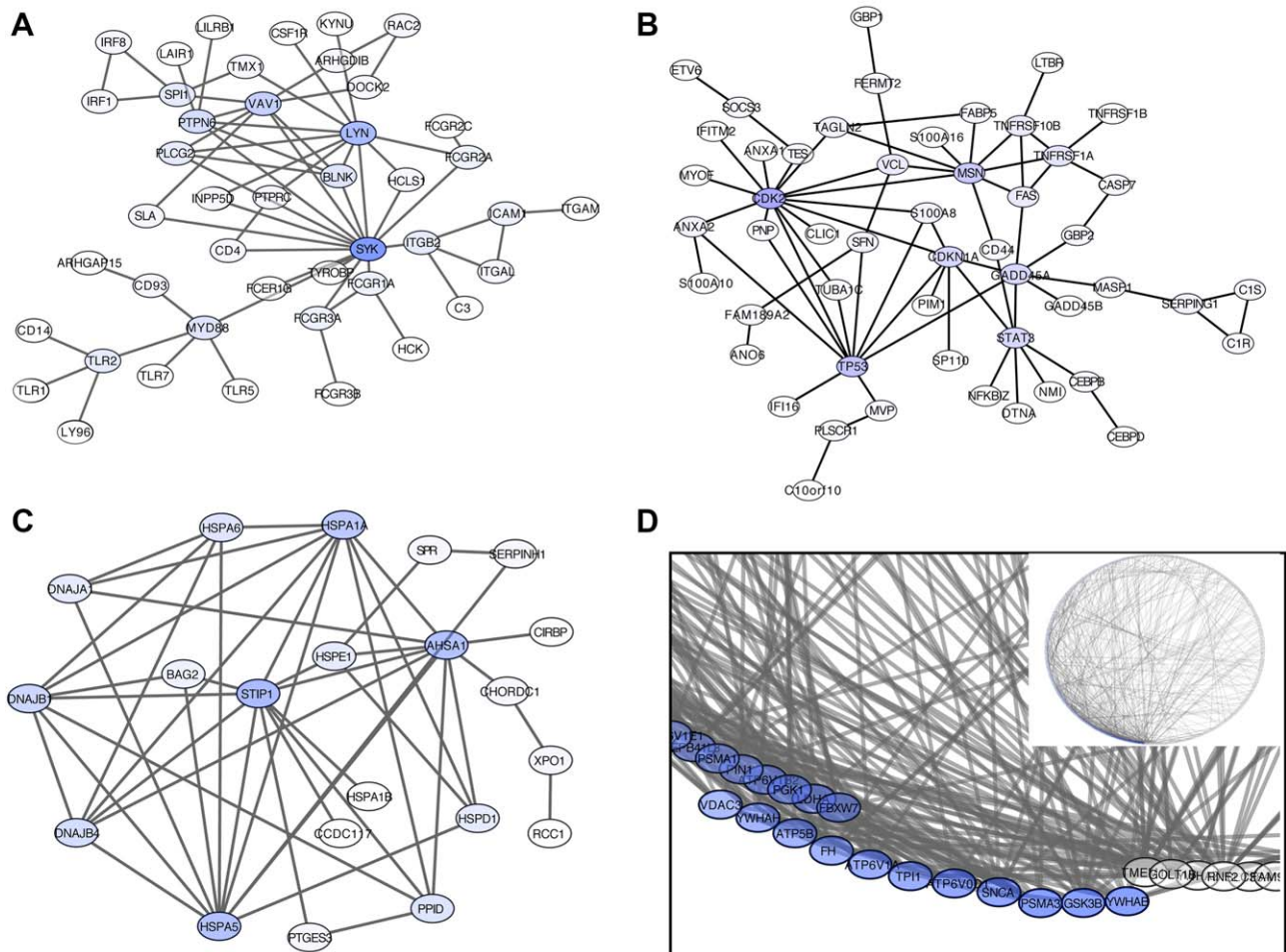


**Figure 4.** Putative subnetworks of protein–protein interactions. **A.** M6-tan module PPI subnetwork showing that spleen tyrosine kinase (encoded by SYK) interacting with 16 partners is the gene with the highest degree of nucleation. **B.** M4-lightcyan module subnetwork showing high degree proteins such as CDK2, MSN and TP53. **C.** M9-salmon PPI subnetwork shows a large connected node related to heat shock proteins encoded by STIP1, DNAJA1, DNAJB1, DNAJB4,

HSPA5, HSAPA6, AHSA1 and HSPA1A, among others. **D.** M5-brown module contains a large PPI subnetwork with several nodes including proteins encoded by YWHAB, GSK3B, PSMA3, ATP6V0D1, TP11, ATP6V1A and SNCA, among others (circular network representation is shown in the small panel proteins ordered by degree, a zoom in the top degree proteins is shown in the larger panel).

identified several hubs and PPI which raise the alert about putative biomarkers and targets for therapeutic intervention.

Lack of comorbidities in the present series implies the selection of a limited number of cases which minimizes the risk of bias. PD and DLB cases have concomitant AD-related pathology which was variable from one case to another. Thal phases were used to evaluate  $\beta$ -amyloid plaques; however, no distinction was made between diffuse and neuritic plaques.

Discussion is centred on selected genes, among those identified by differential expression analysis and weighted correlation networks, whose mRNA expression was assessed with RT-qPCR. The transcriptome is relatively conserved in iLBD and PD as no genes surpass the threshold of significance when  $P$ -values are adjusted for multiple testing. This is in contrast with DLB where hundreds of genes show multiple testing-corrected significant expression differences when compared with MA individuals.

Dyneins are one deregulated cluster in LBDs. Five of seven assessed members are upregulated in iLBD and PD, and three of seven in DLB. Because of their ATP hydrolysis-mediated involvement in cytoplasmic transport (82), early alteration of the cargo transport along neurites may be suggested in the frontal cortex within the LBD spectrum.

Expression of taste and olfactory receptors and down-stream obliged functional signaling pathways in the CNS and their deregulation in neurodegenerative diseases is intriguing. It is possible that these receptors in brain are not involved in the perception of odors and taste but rather correspond to new central chemoreceptors looking for putative ligands or interacting complementary receptors (30). TASRs are significantly upregulated in frontal cortex in PD and DLB (33, 38), and our findings further indicate that deregulation of TASRs in frontal cortex occurs in iLBD as well. Previous studies have shown altered protein synthesis machinery in the frontal cortex in PD and DLB from the nucleolus to the ribosome (36,

**Table 3.** Quantification of the expression of selected genes corresponding to axonema and taste receptors clusters in MA, iLBD, PD and DLB.

Probes	P-value				P-value				P-value			
	MA	iLBD	PD	DLB	MA vs iLBD	Adjusted	MA VS PD	Adjusted	MA vs DLB	Adjusted	Adjusted	
<b>Axonema</b>												
DNAAF1	1.04 ± 0.31	2.18 ± 0.72	2.06 ± 1.03	1.04 ± 0.36	0.000481	0.013524	0.005583	0.078162	0.987973	0.987973	0.987973	
DNAH11	1.16 ± 0.57	3.17 ± 1.94	1.96 ± 0.51	3.27 ± 2.43	0.005601	0.039207	0.003889	0.078162	0.011763	0.011763	0.043544	
DNAH2	1.07 ± 0.41	2.03 ± 0.97	2.40 ± 1.50	1.05 ± 0.38	0.012770	0.061973	0.010576	0.085253	0.899477	0.899477	0.944451	
DNAH5	1.08 ± 0.44	1.76 ± 0.89	1.69 ± 0.83	1.05 ± 0.51	0.064296	0.245494	0.060820	0.196495	0.866887	0.866887	0.944451	
DNAH7	1.08 ± 0.42	1.84 ± 0.69	1.35 ± 0.51	1.67 ± 0.45	0.016352	0.068678	0.245494	0.471895	0.007938	0.007938	0.039284	
DNAH9	1.16 ± 0.63	2.39 ± 2.25	2.36 ± 1.25	1.67 ± 0.56	0.105147	0.339706	0.021719	0.085253	0.084009	0.084009	0.147016	
DNAI1	1.07 ± 0.43	2.13 ± 0.32	3.09 ± 2.22	2.96 ± 1.44	0.000644	0.013524	0.008326	0.085253	0.000592	0.000592	0.021154	
TAS2R4	1.03 ± 0.27	1.48 ± 1.12	1.33 ± 0.80	1.82 ± 0.78	0.203630	0.503086	0.247183	0.471895	0.004187	0.004187	0.035171	
TAS2R5	1.03 ± 0.25	0.61 ± 0.33	1.14 ± 0.67	2.25 ± 1.03	0.013280	0.061973	0.639661	0.814114	0.001261	0.001261	0.021154	
TAS2R14	1.15 ± 0.57	0.89 ± 0.54	2.44 ± 2.31	2.51 ± 1.59	0.427225	0.690133	0.077225	0.231675	0.012441	0.012441	0.043544	
TAS2R50	1.08 ± 0.40	0.68 ± 0.42	0.65 ± 0.65	1.54 ± 1.15	0.091428	0.319998	0.089294	0.250023	0.229848	0.229848	0.321787	
TAS2R10	1.13 ± 0.50	1.49 ± 1.09	4.50 ± 3.33	1.68 ± 0.64	0.371381	0.628649	0.002611	0.078162	0.038324	0.038324	0.080480	
TAS2R13	1.11 ± 0.49	7.27 ± 5.99	0.99 ± 0.50	1.63 ± 0.62	0.002092	0.021966	0.625557	0.814114	0.042350	0.042350	0.080850	

Green, indicates downregulation; Red, indicates upregulation.

Data are expressed as mean values ± SD; significant comparisons between groups are expressed by P-values. Upregulated and downregulated genes are represented by different colors. P-values have been adjusted using the BH method in each contrast and are indicated next to nominal P-values.

38). Nuclear alterations include increased nucleolar stress and altered synthesis of ribosomal RNAs, in addition to altered production of mRNAs. Our findings show altered mRNA expression of different molecules involved in RNA and DNA metabolism such as KAT2A which is upregulated in PD, and PNPT1, PAPOLA, RELA and DOT1Ls which are upregulated in DLB. PNPT1 and RELA are also upregulated in iLBD. Therefore, genes which encode proteins involved in the acetylation and methylation of histones, RNA processing and the modulation of NF-κB-mediated gene transcription are abnormally regulated in DLB and, to a lesser degree, in other disorders within the LBD spectrum. A primary effect of α-synuclein can be postulated, as α-synuclein is abnormally localized in the nucleus in neurons, and probably also in glial cells, in the frontal cortex in PD (36).

Another deregulated cluster in LBD is related to innate inflammatory responses. This has been the subject of two detailed studies in PD and DLB (34, 38). An interesting aspect was the downregulation of cytokines and several mediators of the inflammatory response in the substantia nigra at early stages of PD (34) and the relatively low inflammatory response in the frontal cortex in DLB (38), which is in line with previous observations pointing out the relatively low inflammatory response and enhanced dystrophic microglia in DLB (2, 88, 90). This is further supported in the present study by downregulation of AIF1, which encodes the microglial marker IBA-1 in the frontal cortex in iLBD, thus suggesting early microglial alteration in LBDs.

Another DLB-associated module is related to heat-shock/chaperone proteins and is globally upregulated in DLB. Three out of ten assessed genes are upregulated in the frontal cortex in PD and six out of ten in DLB. These include DNAJA1, DNAJ4 and DNAJB1, the products of which act as heat shock protein 70 cochaperones, and chaperones HSPA4, HSPA6 and HSPD1.

Moreover, STIP1, a copartner in the HSP70/HSP90 activity in protein folding, is the top hub gene in this module and PPI together with HSPA1A and HSPA5. DNAJA1 and DNAJB1 are also among the top hub genes in this module. Importantly, the expression of this gene is increased in PD and DLB but significantly upregulated only in PD. Refolding and clearance of α-synuclein aggregates requires chaperones and the proteasome system (55). Our findings are consistent with the presence of abnormally aggregated α-synuclein in the cortex in DLB and also with previous observations of increased folding proteins and unfolded protein response in DLB (3, 16).

We found a large gene coexpression module downregulated in DLB that is enriched in neuronal markers and in genes mainly involved in synaptic transmission. Synapses are altered in the cortex in PD and DLB (19, 20, 74, 85, 86). α-synuclein is abundant in the pre-synaptic terminals, where it plays a role in synaptic function. Abnormal folding and oligomerization and formation of certain types of aggregates may directly produce synaptic damage, and may do so indirectly by exerting toxicity on mitochondria, lysosomes and cytoskeleton (56, 74, 85). Notably, a top degree gene of the PPI subnetwork from this module is α-synuclein. In spite of being a PPI hub, SNCA is not a DEG between DLB and CTL as assessed by Limma, which highlights the importance of the present higher-complexity level study in revealing genes otherwise veiled in conventional differential expression methods.

Gene downregulation related to neurotransmission in the frontal cortex in DLB particularly involves GAD1, the product of which

**Table 4.** Quantification of the expression of selected genes corresponding to RNA/DNA processing, chaperones and neurotransmitters and synapses in MA, iLBD, PD and DLB.

Probes	MA	iLBD	PD	DLB	P-value			P-value				
					MA vs iLBD	Adjusted	MA vs PD	Adjusted	MA vs DLB	Adjusted		
											MA vs iLBD	MA vs PD
<b>RNA/DNA</b>												
KAT2A	1.08 ± 0.39	1.38 ± 0.80	1.68 ± 0.75	1.65 ± 1.22	0.318894	0.608798	0.032546	0.113911	0.162525	0.252817		
PNPT1	1.03 ± 0.26	1.73 ± 0.45	1.63 ± 0.74	2.18 ± 0.99	0.001300	0.018200	0.020982	0.106943	0.001511	0.021154		
PAPOLA	1.01 ± 0.18	1.02 ± 0.55	1.01 ± 0.33	1.52 ± 0.68	0.966720	0.990299	0.987272	0.997676	0.029792	0.069238		
RELA	1.01 ± 0.14	1.42 ± 0.39	1.62 ± 0.79	2.39 ± 1.84	0.009412	0.056472	0.027832	0.106943	0.029333	0.069238		
DOT1L	1.01 ± 0.16	1.28 ± 0.62	1.24 ± 0.60	1.34 ± 0.48	0.179901	0.472240	0.241060	0.471895	0.046556	0.085015		
DNAJA1	1.02 ± 0.19	1.24 ± 0.58	1.32 ± 0.36	1.51 ± 0.75	0.249723	0.525382	0.027383	0.106943	0.041181	0.080850		
DNAJA4	1.28 ± 0.76	1.62 ± 1.15	1.75 ± 0.83	2.53 ± 1.19	0.479652	0.719478	0.199588	0.471895	0.008306	0.039284		
DNAJB1	1.21 ± 0.65	1.13 ± 0.58	1.14 ± 0.54	2.47 ± 0.54	0.827989	0.921038	0.822303	0.933425	0.020325	0.056910		
DNAJB4	1.21 ± 0.73	1.32 ± 0.70	1.13 ± 0.28	1.64 ± 0.82	0.788308	0.921038	0.776413	0.905815	0.223143	0.321787		
HSPA1A	1.06 ± 0.40	1.16 ± 0.55	1.28 ± 0.88	1.63 ± 1.55	0.727662	0.901719	0.490696	0.775885	0.283092	0.349702		
HSPA4	1.01 ± 0.12	1.05 ± 0.37	1.34 ± 0.42	1.63 ± 0.72	0.727987	0.901719	0.016296	0.097776	0.007965	0.039284		
HSPA5	1.06 ± 0.38	0.84 ± 0.29	1.70 ± 0.78	1.48 ± 0.82	0.270249	0.540498	0.028009	0.106943	0.143620	0.232002		
HSPA6	1.06 ± 0.39	0.86 ± 0.29	1.24 ± 0.91	1.63 ± 0.47	0.374196	0.628649	0.557809	0.780933	0.017922	0.056910		
HSPD1	1.02 ± 0.22	1.01 ± 0.66	1.17 ± 0.46	1.98 ± 1.28	0.950284	0.990299	0.324922	0.568614	0.018989	0.056910		
HSPF1	1.01 ± 0.13	1.04 ± 0.47	1.25 ± 0.50	1.04 ± 0.29	0.827808	0.921038	0.114919	0.301662	0.721566	0.819075		
GABBR2	1.05 ± 0.32	1.15 ± 0.48	1.05 ± 0.46	0.64 ± 0.32	0.616222	0.862711	0.281410	0.513879	0.012003	0.043544		
GABRA1	1.07 ± 0.40	0.88 ± 0.56	1.05 ± 0.52	0.60 ± 0.50	0.451273	0.701980	0.913177	0.958836	0.031322	0.069238		
GAD1	1.08 ± 0.43	0.73 ± 0.45	1.08 ± 0.45	0.50 ± 0.34	0.161648	0.452614	0.997676	0.997676	0.004059	0.035171		
GRIN2A	1.04 ± 0.28	1.04 ± 0.43	1.18 ± 0.45	1.14 ± 0.51	0.999447	0.999447	0.393711	0.661434	0.560841	0.654315		
GRIN2B	1.03 ± 0.27	0.99 ± 0.81	0.93 ± 0.41	1.19 ± 0.56	0.869824	0.936734	0.534280	0.775885	0.409171	0.491005		
NETO1	1.05 ± 0.32	0.47 ± 0.14	1.12 ± 0.75	0.64 ± 0.44	0.005157	0.039207	0.771798	0.905815	0.027200	0.069238		
RAB3A	1.03 ± 0.25	1.09 ± 0.04	1.14 ± 0.48	0.79 ± 0.53	0.636911	0.862912	0.535730	0.775885	0.218554	0.321787		
RPH3A	1.03 ± 0.25	1.10 ± 0.55	1.13 ± 0.53	0.78 ± 0.41	0.729963	0.901719	0.594324	0.805213	0.117159	0.196827		
SNAP25	1.02 ± 0.22	1.06 ± 0.42	1.23 ± 0.49	0.85 ± 0.43	0.833320	0.921038	0.220065	0.471895	0.263212	0.334997		
STXBP1	1.02 ± 0.20	1.12 ± 0.46	1.22 ± 0.49	0.86 ± 0.39	0.530886	0.768869	0.230966	0.471895	0.262784	0.334997		
SYP	1.02 ± 0.20	0.82 ± 0.31	1.09 ± 0.48	0.69 ± 0.29	0.131839	0.395517	0.674822	0.833604	0.008418	0.039284		
SYT1	1.01 ± 0.18	0.88 ± 0.42	1.15 ± 0.63	0.83 ± 0.48	0.357715	0.628649	0.509828	0.775885	0.238214	0.322742		
SYT13	1.04 ± 0.30	0.83 ± 0.38	1.07 ± 0.45	1.05 ± 0.54	0.246984	0.525382	0.868258	0.958836	0.981224	0.987973		
SYT16	1.03 ± 0.25	0.85 ± 0.36	1.05 ± 0.49	1.00 ± 0.59	0.250182	0.525382	0.895977	0.958836	0.868671	0.944451		

Green, indicates downregulation; Red, indicates upregulation.

Data are expressed as mean values ± SD; significant comparisons between groups are expressed by P-values. Upregulated and downregulated genes are represented by different colors. P-values have been adjusted using the BH method in each contrast and are indicated next to nominal P-values.

catalyzes the synthesis of  $\gamma$ -aminobutyric acid from L-glutamic acid, and GABA receptors GABBR2 and GABRA1, showing that the GABAergic system in frontal cortex is vulnerable to DLB. Other downregulated genes are NETO1, which encodes a protein involved in synaptic N-methyl-D-aspartic acid receptor complexes, and SYP, which encodes SYP, a major synaptic protein. In line with the present findings, loss of post-synaptic GABA receptor markers has been reported in the occipital cortex in DLB (52). SYP expression was previously reported as decreased in the occipital cortex in DLB as well (67). The identification of deregulated M5 top hub gene, ATP6V1A, the product of which mediates the acidification of several intracellular organelles including synaptic vesicles, thereby facilitating synaptic transmission (12), further points to altered synaptic function.

Other altered pathways identified in the M5-brown module, namely energy metabolism and mitochondrial function, and purine metabolism, have been the subject of previous analysis. Mitochondria and energy metabolism is altered in the frontal cortex in PD and DLB (37–39, 51, 68, 69, 76, 92). Moreover, decreased enzymatic activity of complexes I–IV has been demonstrated in a subset of PD cases with dementia (38, 69) and in cases with DLB (37, 68). Abnormal  $\alpha$ -synuclein is localized in mitochondria in the frontal cortex in PD (38) and in the nucleus (36); thus, a possible link between altered nuclear and mitochondrial DNA/RNA processing and aberrant  $\alpha$ -synuclein may be considered. The present study also shows two additional PPIs in module 5. Cytochrome c, somatic (CYCS) encodes a small heme protein localized in the inner membrane of the mitochondria which transports electrons from cytochrome b to the cytochrome oxidase complex (21). Second, TPI1 encodes a protein which participates in glycolysis and gluconeogenesis (93).

Regarding purine metabolism, our previous RT-qPCR studies revealed abnormal expression of several enzymes involved in purine metabolism in PD and DLB (35, 38). No attempt was made to validate other important altered pathways such as those linked to the ubiquitin proteasome system (UPS) in LBDs revealed by microarrays, and interpretation of significantly altered regulation of certain top hub genes in M5 such as GSK3B and YWHAB, and M6 as LAPTM5 remains speculative.

## CONCLUDING COMMENTS

The study of human cases is irreplaceable in the effort to gain understanding of the neurodegenerative diseases that are exclusive to human beings. It can be criticized the limited number of available cases suitable for molecular studies in the present series. This limitation may account for certain discrepancies between the observations obtained with arrays and the subsequent validations with RT-qPCR, and also by the observation of isolated deregulated genes which are apparently disconnected from highly represented deregulated clusters. In spite of these constraints, the present study, using selected samples with no comorbidity and adequate RNA preservation, has documented an extraordinary amount of information. Validation of the present findings should be expected in other independent series.

We used a “network medicine” approach to the study of LBDs aiming at unveiling changes in the transcriptome in frontal cortex area 8 which may affect particular metabolic pathways and

biological functions. This approach is being increasingly used to discover relevant pathogenic effectors in neurodegenerative diseases (83). Here, we show early alteration in the regulation of the axonema and particularly of dyneins, and of taste receptors in iLBD, maintained and augmented along with the progression of the LBD spectrum. Interestingly, innate inflammation is downregulated in iLBD as manifested by decreased AIF1 expression. It is worth mentioning that the expression of several cytokines and mediators of the inflammatory response is also reduced in iLBD (unpublished observations); the small number of cases assessed in this series precludes further evaluations, but our findings provide insights that will allow deepening into the study of reduced innate inflammatory regulation at early stages of LBDs. We have also identified and validated deregulation of several pathways in the frontal cortex in DLB; this includes upregulation of RNA/DNA processing and chaperones, and downregulation of neurotransmission thereby revealing the vulnerability of the GABAergic system. Altered mitochondria and energy metabolism, protein synthesis, and altered purine metabolism regulation were the subject of previous studies. Our approach has also identified robust deregulated modules represented by several genes, hub genes and PPI subnetworks within these modules. These observations reveal potential candidates for further analysis as they may involve key pathogenic molecular events taking place in the frontal cortex in LBDs.

## ACKNOWLEDGMENTS

This study was funded by the Ministerio de Economía y Competitividad, Instituto de Salud Carlos III – Fondos FEDER, a Way to Build Europe FIS (grant PI14/00757 to IF and grants BFU-2012-38236 and BFU-2015-68649-P to AN), by the Spanish National Institute of Bioinformatics of the Instituto de Salud (PT13/0001/0026) and by FEDER (Fondo Europeo de Desarrollo Regional)/FSE (Fondo Social Europeo), and coordinated Intraciber 2014: Rapid Dementias. We wish to thank Gerard Muntané for technical assistance and valuable discussion and T. Yohannan for editorial help.

## AUTHOR'S CONTRIBUTION

GS performed WGCNA, PG-E carried out RT-qPCR, PA-B the analysis of arrays, BL-G performed the gene enrichment score analysis, AN refined the design, IF designed the study, selected the cases, supervised the work and wrote the manuscript which was circulated among all the authors to add comments and suggestions. All the authors agreed with the contents of the manuscript.

## REFERENCES

- Alafuzoff I, Ince PG, Arzberger T, Al-Sarraj S, Bell J, Bodi I *et al* (2009) Staging/typing of Lewy body related alphasynuclein pathology: a study of the BrainNet Europe Consortium. *Acta Neuropathol* **117**: 635–652.
- Bachstetter AD, Van Eldik LJ, Schmitt FA, Neltner JH, Ighodaro ET, Webster SJ *et al* (2015) Disease-related microglia heterogeneity in the hippocampus of Alzheimer's disease, dementia with Lewy bodies, and hippocampal sclerosis of aging. *Acta Neuropathol Commun* **3**:32.



3. Baek JH, Whitfield D, Howlett D, Francis P, Berezcki E, Ballard C *et al* (2016) Unfolded protein response is activated in Lewy body dementias. *Neuropathol Appl Neurobiol* **42**:352–365.
4. Barrachina M, Castaño E, Ferrer I (2006) TaqMan PCR assay in the control of RNA normalization in human post-mortem brain tissue. *Neurochem Int* **49**:276–284.
5. Benita Y, Cao Z, Giallourakis C, Li C, Gardet A, Xavier RJ (2010) Gene enrichment profiles reveal T-cell development, differentiation, and lineage-specific transcription factors including ZBTB25 as a novel NF-AT repressor. *Blood* **115**:5376–5384.
6. Blalock EM, Geddes JW, Chen KC, Porter NM, Markesbery WR, Landfield PW (2004) Incipient Alzheimer's disease: microarray correlation analyses reveal major transcriptional and tumor suppressor responses. *Proc Natl Acad Sci USA* **101**:2173–2178.
7. Botta-Orfila T, Sánchez-Pla A, Fernández M, Carmona F, Ezquerro M, Tolosa E (2012) Brain transcriptomic profiling in idiopathic and LRRK2-associated Parkinson's disease. *Brain Res* **1466**:152–157.
8. Boyle PA, Yu L, Wilson RS, Gamble K, Buchman AS, Bennett DA (2012) Poor decision making is a consequence of cognitive decline among older persons without Alzheimer's disease or mild cognitive impairment. *PLoS One* **7**:e43647.
9. Braak H, Braak E (1991) Neuropathological staging of Alzheimer-related changes. *Acta Neuropathol* **82**:239–259.
10. Braak H, Del Tredici K, Rüb U, de Vos RA, Jansen Steur EN, Braak E (2003) Staging of brain pathology related to sporadic Parkinson's disease. *Neurobiol Aging* **24**:197–211.
11. Braak H, Rüb U, Del Tredici K (2006) Cognitive decline correlates with neuropathological stage in Parkinson's disease. *J Neurol Sci* **248**:255–258.
12. Breton S, Brown D (2013) Regulation of luminal acidification by the V-ATPase. *Physiology* **28**:318–329.
13. Buddhala C, Loftin SK, Kuley BM, Cairns NJ, Campbell MC, Perlmutter JS, Kotzbauer PT (2015) Dopaminergic, serotonergic, and noradrenergic deficits in Parkinson disease. *Ann Clin Transl Neurol* **2**:949–959.
14. Burke RE, Dauer WT, Vonsattel JP (2008) A critical evaluation of the Braak staging scheme for Parkinson's disease. *Ann Neurol* **64**:485–491.
15. Cahoy JD, Emery B, Kaushal A, Foo LC, Zamanian JL, Christopherson KS *et al* (2008) A transcriptome database for astrocytes, neurons, and oligodendrocytes: a new resource for understanding brain development and function. *J Neurosci* **28**:264–278.
16. Cantuti-Castelvetri I, Klucken J, Ingelsson M, Ramasamy K, McLean PJ, Frosch MP *et al* (2005) Alpha-synuclein and chaperones in dementia with Lewy bodies. *J Neuropathol Exp Neurol* **64**:1058–1066.
17. Colom-Cadena M, Gelpi E, Charif S, Belbin O, Blesa R, Martí MJ *et al* (2013) Confluence of  $\alpha$ -synuclein, tau, and  $\beta$ -amyloid pathologies in dementia with Lewy bodies. *J Neuropathol Exp Neurol* **72**:1203–1212.
18. Cui S, Sun H, Gu X, Lv E, Zhang Y, Dong P, Fu C *et al* (2015) Gene expression profiling analysis of locus coeruleus in idiopathic Parkinson's disease by bioinformatics. *Neurol Sci* **36**:97–102.
19. Dalfó E, Albasanz JL, Martín M, Ferrer I (2004) Abnormal metabotropic glutamate receptor expression and signaling in the cerebral cortex in diffuse Lewy body disease is associated with irregular alpha-synuclein/phospholipase C (PLC $\beta$ 1) interactions. *Brain Pathol* **14**:388–398.
20. Dalfó E, Barrachina M, Rosa JL, Ambrosio S, Ferrer I (2004) Abnormal alphasynuclein interactions with rab3a and rabphilin in diffuse Lewy body disease. *Neurobiol Dis* **16**:92–97.
21. Delgado JY, Owens GC (2012) The cytochrome c gene proximal enhancer drives activity-dependent reporter gene expression in hippocampal neurons. *Front Mol Neurosci* **5**:31.
22. Dickson DW, Fujishiro H, DelleDonne A, Menke J, Ahmed Z, Klos KJ *et al* (2008) Evidence that incidental Lewy body disease is pre-symptomatic Parkinson's disease. *Acta Neuropathol* **115**:437–444.
23. Dickson DW, Uchikado H, Fujishiro H, Tsuboi Y (2010) Evidence in favor of Braak staging of Parkinson's disease. *Mov Disord* **25**:S78–S82.
24. Diez D, Hutchins AP, Miranda-Saavedra D (2014) Systematic identification of transcriptional regulatory modules from protein-protein interaction networks. *Nucleic Acids Res* **42**:e6.
25. Durrenberger PF, Fernando FS, Magliozzi R, Kashefi SN, Bonnet TP, Ferrer I *et al* (2012) Selection of novel reference genes for use in the human central nervous system: a BrainNet Europe Study. *Acta Neuropathol* **124**:893–903.
26. Fabelo N, Martín V, Santpere G, Marín R, Torrent L, Ferrer I, Diaz M (2011) Severe alterations in lipid composition of frontal cortex lipid rafts from Parkinson's disease and incidental Parkinson's disease. *Mol Med* **17**:1107–1118.
27. Falcon S, Gentleman R (2007) Using GStats to test gene lists for GO term association. *Bioinformatics* **23**:257–258.
28. Ferrer I (2009) Early involvement of the cerebral cortex in Parkinson's disease: convergence of multiple metabolic defects. *Prog Neurobiol* **88**:89–103.
29. Ferrer I, Martínez A, Boluda S, Parchi P, Barrachina M (2008) Brain banks: benefits, limitations and cautions concerning the use of post-mortem brain tissue for molecular studies. *Cell Tissue Bank* **9**:181–194.
30. Ferrer I, Garcia-Esparcia P, Carmona M, Carro E, Aronica E, Kovacs G *et al* (2016) Olfactory receptors in non-chemosensory organs: the nervous system in health and disease. *Front Aging Neurosci* **8**:163.
31. Ferrer I, López-Gonzalez I, Carmona M, Dalfó E, Pujol A, Martínez A (2012) Neurochemistry and the non-motor aspects of PD. *Neurobiol Dis* **46**:508–526.
32. Fujishiro H, Ferman TJ, Boeve BF, Smith GE, Graff-Radford NR, Uitti RJ *et al* (2008) Validation of the neuropathologic criteria of the third consortium for dementia with Lewy bodies for prospectively diagnosed cases. *J Neuropathol Exp Neurol* **67**:649–656.
33. Garcia-Esparcia P, Schlüter A, Carmona M, Moreno J, Ansoleaga B, Torrejón-Escribano B *et al* (2013) Functional genomics reveals dysregulation of cortical olfactory receptors in Parkinson disease: novel putative chemoreceptors in the human brain. *J Neuropathol Exp Neurol* **72**:524–539.
34. Garcia-Esparcia P, Llorens F, Carmona M, Ferrer I (2014) Complex deregulation and expression of cytokines and mediators of the immune response in Parkinson's disease brain is region dependent. *Brain Pathol* **24**:584–598.
35. Garcia-Esparcia P, Hernández-Ortega K, Ansoleaga B, Carmona M, Ferrer I (2015) Purine metabolism gene deregulation in Parkinson's disease. *Neuropathol Appl Neurobiol* **41**:926–940.
36. Garcia-Esparcia P, Hernández-Ortega K, Koneti A, Gil L, Delgado-Morales R, Castaño E *et al* (2015) Altered machinery of protein synthesis is region- and stage-dependent and is associated with  $\alpha$ -synuclein oligomers in Parkinson's disease. *Acta Neuropathol Commun* **3**:76.
37. Garcia-Esparcia P, Koneti A, Rodríguez-Oroz MC, Lago B, del Rio JA, Ferrer I (2017) Mitochondrial activity in the frontal cortex area 8 and angular gyrus in Parkinson's disease and Parkinson's disease with dementia. *Brain Pathol* (in press).
38. Garcia-Esparcia P, López Gonzalez I, Grau-Rivera O, García-Garrido MF, Konetti A, Llorens F, *et al* (2017) Dementia with Lewy bodies: age-related molecular pathology in the frontal cortex in typical and rapidly progressive forms. *Front Neurol* (in press).
39. Gatt AP, Duncan OF, Attems J, Francis PT, Ballard CG, Bateman JM (2016) Dementia in Parkinson's disease is associated with enhanced mitochondrial complex I deficiency. *Mov Disord* **31**:352–359.

40. Glaab E, Schneider R (2015) Comparative pathway and network analysis of brain transcriptome changes during adult aging and in Parkinson's disease. *Neurobiol Dis* **74**:1–13.
41. Goedert M (2001) Alpha-synuclein and neurodegenerative diseases. *Nat Rev Neurosci* **2**:492–501.
42. Grison A, Zucchelli S, Urzi A, Zamparo I, Lazarevic D, Pascarella G et al (2014) Mesencephalic dopaminergic neurons express a repertoire of olfactory receptors and respond to odorant-like molecules. *BMC Genomics* **15**:729.
43. Grothe MJ, Schuster C, Bauer F, Heinsen H, Prudlo J, Teipel SJ (2014) Atrophy of the cholinergic basal forebrain in dementia with Lewy bodies and Alzheimer's disease dementia. *J Neurol* **261**:1939–1948.
44. Hawrylycz MJ, Lein ES, Guillozet-Bongaarts AL, Shen EH, Ng L, Miller JA et al (2012) An anatomically comprehensive atlas of the adult human brain transcriptome. *Nature* **489**:391–399.
45. Huang SH, Chang CC, Lui CC, Chen NC, Lee CC, Wang PW, Jiang CF (2015) Cortical metabolic and nigrostriatal abnormalities associated with clinical stage-specific dementia with Lewy bodies. *Clin Nucl Med* **40**:26–31.
46. Ince PG (2011) Dementia with Lewy bodies and Parkinson's disease with dementia. In: *Neurodegeneration, the Molecular Pathology of Dementia and Movement Disorders*. DW Dickson, RO Weller (eds), pp. 224–237. Wiley-Blackwell: Oxford
47. Jellinger KA (2007) Morphological substrates of parkinsonism with and without dementia: a retrospective clinico-pathological study. *J Neural Transm* **72**:91–104.
48. Jellinger KA (2009) Significance of brain lesions in Parkinson disease dementia and Lewy body dementia. *Front Neurol Neurosci* **24**:114–125.
49. Jellinger KA (2011) Parkinson's disease. In: *Neurodegeneration: The Molecular Pathology of Dementia and Movement Disorders*. DW Dickson, RO Weller (eds), pp. 194–233. Wiley-Blackwell: Oxford.
50. Jellinger KA, Attems J (2008) Prevalence and impact of vascular and Alzheimer pathologies in Lewy body disease. *Acta Neuropathol* **115**:427–436.
51. Keeney PM, Xie J, Capaldi RA, Bennett JP (2006) Parkinson's disease brain mitochondrial complex I has oxidatively damaged subunits and is functionally impaired and misassembled. *J Neurosci* **26**:5256–5264.
52. Khundakar AA, Hanson PS, Erskine D, Lax NZ, Roscamp J, Karyka E et al (2016) Analysis of primary visual cortex in dementia with Lewy bodies indicates GABAergic involvement associated with recurrent complex visual hallucinations. *Acta Neuropathol Commun* **4**:66.
53. Kim HJ, Lee JE, Shin SJ, Sohn YH, Lee PH (2011) Analysis of the substantia innominata volume in patients with Parkinson's disease with dementia, dementia with Lewy bodies, and Alzheimer's disease. *J Mov Disord* **4**:68–72.
54. Klein JC, Eggers C, Kalbe E, Weisenbach S, Hohmann C, Vollmar S et al (2010) Neurotransmitter changes in dementia with Lewy bodies and Parkinson disease in vivo. *Neurology* **74**:885–892.
55. Klucken J, Shin Y, Masliah E, Hyman BT, McLean PJ (2004) Hsp70 Reduces  $\alpha$ -synuclein aggregation and toxicity. *J Biol Chem* **279**:25497–25502.
56. Kramer ML, Schulz-Schaeffer WJ (2007) Presynaptic alpha-synuclein aggregates, not Lewy bodies, cause neurodegeneration in dementia with Lewy bodies. *J Neurosci* **27**:1405–1410.
57. Langfelder P, Horvath S (2008) WGCNA: An R package for weighted correlation network analysis. *BMC Bioinformatics* **9**:559.
58. Lein ES, Hawrylycz MJ, Ao N, Ayres M, Bensinger A, Bernard A et al (2006) Genome-wide atlas of gene expression in the adult mouse brain. *Nature* **445**:168–176.
59. Lewis PA, Cookson MR (2012) Gene expression in the Parkinson's disease brain. *Brain Res Bull* **88**:302–312.
60. Liang WS, Dunckley T, Beach TG, Grover A, Mastrieni D, Ramsey K et al (2008) Altered neuronal gene expression in brain regions differentially affected by Alzheimer's disease: a reference data set. *Physiol Genomics* **33**:240–256.
61. Lim S, Chun Y, Lee JS, Lee SJ (2016) Neuroinflammation in synucleinopathies. *Brain Pathol* **26**:404–409.
62. Lim SM, Katsifis A, Villemagne VL, Best R, Jones G, Saling M et al (2009) The 18F-FDG PET cingulate island sign and comparison to 123I-beta-CIT SPECT for diagnosis of dementia with Lewy bodies. *J Nucl Med* **50**:1638–1645.
63. Marin R, Fabelo N, Martín V, Garcia-Esparcia P, Ferrer I, Quinto-Aleman D, Diaz M (2016) Anomalies occurring in lipid profiles and protein distribution in frontal cortex lipid rafts in dementia with Lewy bodies disclose neurochemical traits partially shared by Alzheimer's and Parkinson's diseases. *Neurobiol Aging* **49**:52–59.
64. McKeith I, Mintzer J, Aarsland D, Burn D, Chiu H, Cohen-Mansfield J et al (2004) Dementia with Lewy bodies. *Lancet Neurol* **3**:19–28.
65. Milber JM, Noorigian JV, Morley JF, Petrovitch H, White L, Ross GW, Duda JE (2012) Lewy pathology is not the first sign of degeneration in vulnerable neurons in Parkinson disease. *Neurology* **79**:2307–2314.
66. Miller J, Woltjer RL, Goodenbour JM, Horvath S, Geschwind DH (2013) Genes and pathways underlying regional and cell type changes in Alzheimer's disease. *Genome Med* **5**:48.
67. Mukaetova-Ladinska EB, Andras A, Milne J, Abdel-All Z, Borr I, Jaros E et al (2013) Synaptic proteins and choline acetyltransferase loss in visual cortex in dementia with Lewy bodies. *J Neuropathol Exp Neurol* **72**:53–60.
68. Navarro A, Boveris A (2009) Brain mitochondrial dysfunction and oxidative damage in Parkinson's disease. *J Bioenerg Biomembr* **41**:517–521.
69. Navarro A, Boveris A, Bández MJ, Sánchez-Pino MJ, Gómez C, Muntané G, Ferrer I (2009) Human brain cortex: mitochondrial oxidative damage and adaptive response in Parkinson disease and in dementia with Lewy bodies. *Free Radic Biol Med* **46**:1574–1580.
70. Nelson PT, Kryscio RJ, Jicha GA, Abner EL, Schmitt FA, Xu LO et al (2009) Relative preservation of MMSE scores in autopsy-proven dementia with Lewy bodies. *Neurology* **73**:1127–1133.
71. Nelson PT, Abner EL, Schmitt FA, Kryscio RJ, Jicha GA, Smith CD et al (2010) Modeling the association between 43 different clinical and pathological variables and the severity of cognitive impairment in a large autopsy cohort of elderly persons. *Brain Pathol* **20**:66–79.
72. Odunuga OO, Longshaw VM, Blatch GL (2004) Hop: more than an Hsp70/Hsp90 adaptor protein. *BioEssays* **26**:1058–1068.
73. Oldham MC, Konopka G, Iwamoto K, Langfelder P, Kato T, Horvath S, Geschwind DH (2009) Functional organization of the transcriptome in human brain. *Nat Neurosci* **11**:1271–1282.
74. Overk CR, Masliah E (2014) Pathogenesis of synaptic degeneration in Alzheimer's disease and Lewy body disease. *Biochem Pharmacol* **88**:508–516.
75. Parachikova A, Agadjanyan MG, Cribbs DH, Blurton-Jones M, Perreau V, Rogers J et al (2007) Inflammatory changes parallel the early stages of Alzheimer disease. *Neurobiol Aging* **28**:1821–1833.
76. Parker WD, Parks JK, Swerdlow RH (2008) Complex I deficiency in Parkinson's disease frontal cortex. *Brain Res* **1189**:215–218.
77. Parkkinen L, Kauppinen T, Pirttilä T, Autere JM, Alafuzoff I (2005)  $\alpha$ -synuclein pathology does not predict extrapyramidal symptoms or dementia. *Ann Neurol* **57**:82–91.
78. Parkkinen L, Pirttilä T, Alafuzoff I (2008) Applicability of current staging/categorization of alpha-synuclein pathology and their clinical relevance. *Acta Neuropathol* **115**:399–407.
79. Price DL, Rockenstein E, Ubhi K, Phung V, MacLean-Lewis N, Askay D et al (2010) Alterations in mGluR5 expression and signaling in Lewy body disease and in transgenic models of alpha-synucleinopathy—implications for excitotoxicity. *PLoS One* **5**:e14020.

80. Ravid R, Ferrer I (2012) Brain banks as key part of biochemical and molecular studies on cerebral cortex involvement in Parkinson's disease. *FEBS J* **279**:1167–1176.
81. Ritchie ME, Phipson B, Wu D, Hu Y, Law CW, Shi W, Smyth GK (2015) Limma powers differential expression analyses for RNA-sequencing and microarray studies. *Nucleic Acids Res* **43**:e47.
82. Roberts AJ, Kon T, Knight PJ, Sutoh K, Burgess SA (2013) Functions and mechanics of dynein motor proteins. *Nat Rev Mol Cell Biol* **14**: 713–726.
83. Santiago JA, Potashkin JA (2014) A network approach to clinical intervention in neurodegenerative diseases. *Trends Mol Med* **20**:694–703.
84. Schneider JA, Arvanitakis Z, Yu L, Boyle PA, Leurgans SE, Bennette DA (2012) Cognitive impairment, decline and fluctuations in older community-dwelling subjects with Lewy bodies. *Brain* **135**:3005–3014.
85. Schulz-Schaeffer WJ (2010) The synaptic pathology of  $\alpha$ -synuclein aggregation in dementia with Lewy bodies, Parkinson's disease and Parkinson's disease dementia. *Acta Neuropathol* **120**:131–143.
86. Scott DA, Tabarean I, Tang Y, Cartier A, Masliah E, Roy S (2010) A pathologic cascade leading to synaptic dysfunction in alpha-synuclein-induced neurodegeneration. *J Neurosci* **30**:8083–8095.
87. Shannon P, Markiel A, Ozier O, Baliga NS, Wang JT, Ramage D *et al* (2005) Cytoscape: a software environment for integrated models of biomolecular interaction networks. *Am Assoc Cancer Res Educ B* **13**: 2498–2504.
88. Shepherd CE, Thiel E, McCann H, Harding AJ, Halliday GM (2000) Cortical inflammation in Alzheimer disease but not dementia with Lewy bodies. *Arch Neurol* **57**:817–822.
89. Shimada H, Hirano S, Shinotoh H, Aotsuka A, Sato K, Tanaka N *et al* (2009) Mapping of brain acetylcholinesterase alterations in Lewy body disease by PET. *Neurology* **73**:273–278.
90. Streit WJ, Xue QS (2016) Microglia in dementia with Lewy bodies. *Brain Behav Immun* **55**:191–201.
91. Thal DR, Rüb U, Orantes M, Braak H (2002) Phases of A beta-deposition in the human brain and its relevance for the development of AD. *Neurology* **58**:1791–1800.
92. Thomas RR, Keeney PM, Bennett JP (2012) Impaired complex-I mitochondrial biogenesis in Parkinson disease frontal cortex. *J Parkinsons Dis* **2**:67–76.
93. Trentham DR, McMurray CH, Pogson CI (1969) The active chemical state of D-glyceraldehyde 3-phosphate in its reactions with D-glyceraldehyde 3-phosphate dehydrogenase, aldolase and triose phosphate isomerase. *Biochem J* **114**:19–24.
94. Walker DG, Lue LF, Serrano G, Adler CH, Caviness JN, Sue LL, Beach TG (2016) Altered expression patterns of inflammation-associated and trophic molecules in substantia nigra and striatum brain samples from Parkinson's disease, incidental Lewy body disease and normal control cases. *Front Neurosci* **9**:507.

## SUPPORTING INFORMATION

Additional Supporting Information may be found in the online version of this article at the publisher's web-site:

**Supplementary Table 1.** TaqMan probes used in the study, gene abbreviation, full name of the genes and references.

**Supplementary Table 2.** Number of DEGs for different thresholds for each comparison of iLBD, PD, DLB and middle aged individuals.

**Supplementary Table 3.** Gene ontology analysis comparing upregulated and downregulated genes in the different categories.

**Supplementary Table 4.** Fifty top upregulated and top downregulated genes, frontal cortex area 8 in DLB.

**Supplementary Table 5.** Top 20 hub genes per modules.

**Supplementary Table 6.** Enrichment of modules in neuronal and glial cell markers, and commonalities with neurological diseases such as Alzheimer's disease and autism.

**Supplementary Table 7.** Identification of enriched GO among genes in each module.